

**FOURIER TRANSFORM INFRARED SPECTROSCOPIC AND DENSITY
FUNCTIONAL THEORETICAL STUDIES OF SILICON-CARBON MOLECULES**

by

TINA HUONG LÊ

Bachelor of Arts, 2008
Reed College
Portland, Oregon

Submitted to the Graduate Faculty of the
College of Science and Engineering
Texas Christian University
in partial fulfillment of the requirements
for the degree of

Doctor of Philosophy

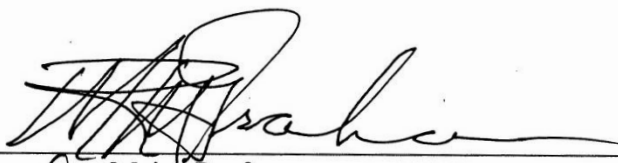
May 2014

FOURIER TRANSFORM INFRARED SPECTROSCOPIC AND DENSITY
FUNCTIONAL THEORETICAL STUDIES OF SILICON-CARBON MOLECULES

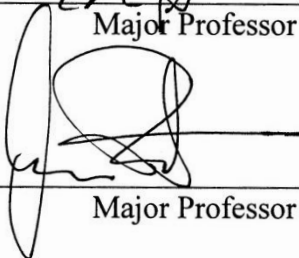
By

Christina "Tina" Huong Lê

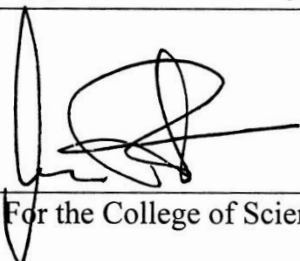
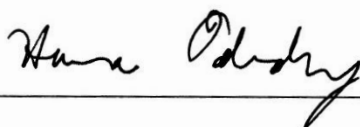
Dissertation Approved:



Major Professor



Major Professor



For the College of Science and Engineering

Copyright by
Tina Huong Lê
2014

I would like to dedicate this dissertation to my friends, mentors and family.

ACKNOWLEDGEMENTS

To Dr. W. R. M. Graham and Dr. C.M.L Rittby, for their patience, support, encouragement, and guidance.

Thanks to M. Murdock, D. Yale, and G. Katchinska for their help in building, repairing and maintaining lab equipment, and for their patience and encouragement.

Support of this research by the Welch Foundation, the W. M. Keck Foundation, and the TCU Research and Creative Activities Fund, the Graduate Student Senate and the Office of Graduate Studies is also gratefully acknowledged.

TABLE OF CONTENTS

ACKNOWLEDGEMENTS	iii
LIST OF FIGURES	vi
LIST OF TABLES	ix
CHAPTER I INTRODUCTION	1
1.1 POTENTIAL ASTROPHYSICAL APPLICATIONS.....	1
1.2 PREVIOUS SILICON-CARBON RESEARCH.....	2
1.3 FOCUS OF THE PRESENT RESEARCH.....	7
CHAPTER II EXPERIMENTAL PROCEDURES.....	10
2.1 FOURIER TRANSFORM INFRARED SPECTROSCOPY.....	10
2.2 SAMPLE PREPARATION: MATRIX TRAPPING AND LASER ABLATION	10
2.2.1. <i>Rod Preparation</i>	14
2.2.2. <i>Laser Ablation</i>	15
2.2.3. <i>Matrix Trapping</i>	15
2.3 ISOTOPIC SHIFT PATTERNS	16
CHAPTER III FTIR ISOTOPIC STUDY OF SIC₅.....	20
3.1 INTRODUCTION.....	20
3.2 EXPERIMENT.....	22
3.3 RESULTS AND ANALYSIS	23
3.4 CONCLUSION	28

CHAPTER IV FTIR IDENTIFICATION OF ν_5 MODE OF SIC₅SI.....	32
4.1 INTRODUCTION.....	32
4.2 EXPERIMENTAL PROCEDURE	34
4.3 RESULTS AND ANALYSIS	35
4.4 CONCLUSION	41
CHAPTER V UNIDENTIFIED ABSORPTIONS.....	47
5.1 1848.2 CM ⁻¹	47
5.2 THE 1985 - 2065 CM ⁻¹ REGION.....	63
CHAPTER VI CONCLUSIONS AND FUTURE WORK.....	67
6.1 INTRODUCTION.....	67
6.2 LINEAR SIC ₅	67
6.3 LINEAR SIC ₅ SI.....	68
6.4 FUTURE WORK.....	68
6.4.1. <i>Identification of the Carriers for Unidentified Bands.....</i>	69
6.4.2. <i>Producing Rods with Higher Si Enrichment.....</i>	69
REFERENCES	70

ABSTRACT

VITA

LIST OF FIGURES

Figure 1.1	The average deviations of neon- and argon-matrix frequencies and of unrestricted calculations of vibrational fundamentals of free radicals from observed gas-phase values. In each group, top = numerical average, middle = absolute average, and bottom = standard deviation.) 9
Figure 2.1	Diagram of the Michelson interferometer.....12
Figure 2.2	Top down view showing laser ablation of a sample rod, the resulting vapor, and the gold mirror on which molecules are trapped. The rod is continually rotated and translated vertically during ablation.....12
Figure 2.3	Top view of experimental setup. Not to scale.....13
Figure 2.4	Simulation of the isotopic shifts of a vibrational mode of SiC ₅18
Figure 2.5	Simulation of the isotopic shifts of a vibrational mode of C ₆ . The numbers 1, 2, and 3 identify the pairs of carbon atoms responsible for the shifts.19
Figure 3.1	Comparison of the FTIR spectra produced by the ablation of (a) graphite rod, (b) a sintered, mixed 5% Si / 95% C rod, (c) a DFT simulation at the B3LYP/cc-pVDZ level of the ^{29,30} Si-isotopic shifts for the ν ₄ (σ) mode of linear, triplet SiC ₅ . Isotopomer frequencies in the spectrum in (b, c) are labeled according to the list in Table 3.3.25
Figure 3.2	Comparison of isotopic shift spectra of the ν ₄ (σ) mode of linear SiC ₅ produced by (a) the ablation of a sintered, mixed 5% Si /10% ¹³ C rod, with a DFT simulation for 10% ¹³ C enrichment, calculated at the (b) B3LYP/cc-pVDZ level. ¹³ C-

	isotopic shift frequencies and isotopomers in the spectra are labeled according to the list in.....	29
Figure 3.3.	FTIR spectra, from 900 to 2300 cm^{-1} , obtained after (a) ablation of sintered, mixed 5% Si / 95% ^{12}C rod and (b) ablation of ablation of sintered, mixed 5% Si / 10% ^{13}C rod. These spectra are shown to emphasize the difficulty of finding experimental candidates for the ν_1 , and ν_2 modes of SiC_5	31
Figure 4.1	Comparison of the FTIR spectra produced by the ablation of (a) graphite rod, (b) a sintered, mixed 30% Si / 70% ^{12}C rod, (c) a DFT simulation at the B3LYP/cc-pVDZ level of the $^{29,30}\text{Si}$ -isotopic shifts for the $\nu_5(\sigma_u)$ mode of linear, triplet SiC_5Si	36
Figure 4.2	Comparison of isotopic shift spectra of the $\nu_5(\sigma_u)$ mode of linear SiC_5 produced by (a) the ablation of a sintered, mixed 30% Si / 10% ^{13}C / 60% ^{12}C rod, (b) the ablation of a sintered, mixed 30% Si / 20% ^{13}C / 50% ^{12}C rod, and with (c) a DFT simulation for 20% ^{13}C enrichment, calculated at the B3LYP/cc-pVDZ level.	38
Figure 4.3	FTIR spectra, from 1550 to 2200 cm^{-1} , obtained after (a) ablation of sintered, mixed 30% Si / 70% ^{12}C rod and (b) ablation of sintered, mixed 30% Si / 20% ^{13}C rod. These spectra are shown to emphasize the difficulty of analyzing the isotopic shift pattern of the observed candidate, 2021.0 cm^{-1} for the ν_4 mode of SiC_5Si	44
Figure 4.4	FTIR spectra, from 1965 to 2025 cm^{-1} , obtained after (a) ablation of sintered, mixed 30% Si / 20% ^{13}C experiment and (b) a DFT simulation for Si / 20% ^{13}C	

enrichment, calculated at the B3LYP/cc-pVDZ level, which has been scaled by $2021.3/2155.0 \approx 0.9379582$. Absorptions that are identified to be $^{12,13}C_n$ are marked by green squares. Absorptions that are identified to be Si_nC_m are marked by blue squares. Candidates for ν_4 isotopomers of SiC_5Si are marked by red circles.46

Figure 5.1 Comparison of FTIR spectra produced by the ablation of (a) a graphite rod, (b) a soft 30% Si / 70% ^{12}C (by mol) rod, (c) a soft 30% Si / 60% ^{12}C / 10% ^{13}C rod, and (d) a soft 30% Si / 50% ^{12}C / 20% ^{13}C rod.....48

Figure 5.2 Comparison of the ^{13}C shift spectra observed for (a) the 1848.2 cm^{-1} absorption and for (b) the $\nu_4(\sigma_u) = 1957.2 cm^{-1}$ band of C_6 , produced in both cases by the ablation of a soft, 30% Si / 60% ^{12}C / 10% ^{13}C rod. The spectrum in (b) has been scaled by 1848.2 / 1952.7 cm^{-1} . The differences between corresponding singly-substituted, isotopomer bands are 2.3, 1.3 and 0.6 cm^{-1} (from low to high frequency bands).....49

Figure 5.3. Comparison of the DFT-B3LYP/cc-pVDZ calculations for the vibrational modes of SiC_nSi , where n is even.56

Figure 5.4. Comparison of the DFT-B3LYP/cc-pVDZ calculations for the vibrational modes of SiC_nSi , where n is odd.....57

Figure 5.5. Comparison of the ^{13}C shift spectra simulated using DFT-B3LYP/cc-pVDZ for (a) $OSiC_6SiO$ (b) $SiOC_6OSi$ (c) NC_6N (d) $NSiC_6SiN$ with (e) the observed ^{13}C shift spectrum for 1848.2 cm^{-1} absorption.....62

Figure 5.6. Spectrum in the region 1985-2065 cm^{-1} produced from the laser ablation of a 30% Si/ 10% ^{13}C rod. There are four unidentified, potential Si_nC_m bands at 1992.1, 1992.9, 2045.0 and 2060.1 cm^{-1}65

LIST OF TABLES

Table 1.1.	A listing of molecules observed in the interstellar medium and/or circumstellar shells as recorded by the Cologne Database for Molecular Spectroscopy (CDMS) in May 2009 (Ref. 2). Tentative identifications are denoted by “?”.....	3
Table 1.2	Three Predicted Vibrational Fundamentals of SiC ₅ . Please refer to the glossary for the definitions of acronyms.....	9
Table 3.1.	DFT-B3LYP/cc-pVDZ predicted vibrational modes, frequencies (cm ⁻¹), and infrared intensities (km/mol) for linear, triplet (³ Σ) SiC ₅	26
Table 3.2.	DFT-B3LYP/cc-pVDZ predicted bond lengths for linear, triplet (³ Σ) SiC ₅	26
Table 3.3	Comparison of observed ²⁹ Si, ³⁰ Si and ¹³ C isotopic shift frequencies (cm ⁻¹) to DFT-B3LYP/cc-PVDZ predicted isotopic frequencies for the ν ₄ (σ) mode of linear triplet (³ Σ) SiC ₅	30
Table 4.1.	DFT-BVWN5/cc-PVDZ predicted vibrational modes, frequencies (cm ⁻¹), and infrared intensities (km/mol) for linear, singlet (¹ Σ _g ⁻) SiC ₅ Si.....	39
Table 4.2.	Comparison of observed ²⁹ Si, ³⁰ Si and ¹³ C isotopic shift frequencies (cm ⁻¹) to DFT-B3LYP/cc-pVDZ predicted isotopic frequencies for the ν ₅ (σ _u) mode of linear, singlet (¹ Σ _g ⁻) SiC ₅ Si.	43
Table 4.3.	Comparison of observed ¹³ C isotopomer frequencies (cm ⁻¹) to DFT-B3LYP/cc-pVDZ predicted singly-substituted isotopic frequencies for the ν ₄ (σ _u) mode of linear, singlet (¹ Σ _g ⁻) SiC ₅ Si.....	45
Table 5.1.	DFT-B3LYP/cc-pVDZ predicted vibrational modes, frequencies (cm ⁻¹), and infrared intensities (km/mol) for linear, triplet (³ Σ _g ⁻) SiC ₆ Si.....	52

Table 5.2	Comparison of DFT- B3LYP/cc-pVDZ calculations and observed vibrational modes for previously reported centrosymmetric molecules.....	53
Table 5.3	Candidate species for the 1848.2 cm ⁻¹ band. They are listed with the corresponding DFT-B3LYP/cc-pVDZ predicted vibrational mode, frequency, and multiplicity. These candidate species were calculated to have an isotopic shift pattern similar to that of 1848.2 cm ⁻¹	59
Table 5.4	Differences between the calculated isotopomer shift bands for different candidate species and the corresponding observed isotopomer bands belonging to 1848.2 cm ⁻¹ . These candidate species were calculated to have an isotopic shift pattern similar to that of 1848.2 cm ⁻¹ . The numerical similarities between these simulations and the observed isotopic shift pattern, leaves the question of what carrier is responsible for the 1848.2 cm ⁻¹ absorption open.....	59

CHAPTER I

INTRODUCTION

1.1 POTENTIAL ASTROPHYSICAL APPLICATIONS

For a long time, scientists have been exploring tinier and tinier structures (from molecules, to atoms to quarks), but due to the complicated nature of these systems, so much is still unknown about them. Research on small structures is motivated by several applications. In the present work on molecular investigations, there is the potential application to studies of chemical processes in astrophysical environments. Ziurys and Apponi¹ emphasized this,

“The use of molecular lines as tracers of the dense interstellar medium has revolutionized our knowledge of star and solar system formation, galactic structure, stellar nucleosynthesis, and even cosmology. Hence, laboratory and theoretical molecular data has aided both in the chemical and physical knowledge of the universe”.

For example, the carbon star IRC + 10216.1, also known as CW Leonis, has many different carbon-containing species, in particular the silicon-carbon species, SiC, SiC₂, SiC₃, and SiC₄ have been identified in its circumstellar shell. This star is surrounded by dense clouds of gas and dust, which absorb high energy light such as the visible and the ultraviolet. Its many properties were detected using radio and infrared astronomy, because lower energy radiation, such as infrared, easily passes through the dense media.

Furthermore, the Cologne Database for Molecular Spectroscopy (CDMS) has recorded 180 molecules (listed in Table 1.1) as of May 2013, to have been observed in interstellar medium

or circumstellar shells.² Among the molecules listed are carbon chains (*e.g.* C₃, C₄, C₅), molecules with carbon chain backbones (*e.g.* CCCN, HC₄N, C₅N, HC₉), and around a dozen Si-bearing species (*e.g.* SiC₃, SiC₂, SiO, SiN). In addition to astrophysical applications, molecular information is also important to chemical physicists and computational theorists who want to determine their structures, chemical bond properties and create models to predict undiscovered molecules.

1.2 PREVIOUS SILICON-CARBON RESEARCH

Astronomers, experimentalists and theorists have produced a great deal of research on Si_{*n*}C_{*m*} species and the present work is part of this on-going research. The history of SiC₂ exemplifies this research. In 1926, Merrill³ and Sanford⁴ reported its blue-green absorption band in certain carbon-rich stars (however, they did not yet know that it was SiC₂). Thirty years later the molecule's identification was made by Kleman⁵ in the laboratory, and then almost 30 years after that in 1985, Shepherd and Graham determined the T-shaped structure of SiC₂ with ionic bonding.⁶ Weltner and McLeod were the first to matrix trap a Si-C molecule in 1964, which was SiC₂ but did not determine the molecule's structure. Vibrational modes for Ne, Ar, and gas phase measurements were reported by Bondybey,⁷ Presilla-Márquez *et al.*,⁸ and Butenhoff and Rohlffing, respectively.⁹ Similarly to SiC₂, SiC₄ was also detected in space, and this time by Ohishi *et al.*¹⁰ via its rotational spectrum; before its vibrational spectrum was measured in an Ar matrix by Withey *et al.* SiC was first identified by Bernath *et al.*¹¹ in the laboratory and then by Cernicharo *et al.* in the envelope of IRC+10216.¹²

Table 1.1. A listing of molecules observed in the interstellar medium and/or circumstellar shells as recorded by the Cologne Database for Molecular Spectroscopy (CDMS) in May 2009 (Ref. 2). Tentative identifications are denoted by “?”.

2 atoms	3	4	5	6	7	8	9	10	11	12
H ₂	C ₃	c-C ₃ H	C ₅	C ₅ H	C ₆ H	CH ₃ C ₃ N	CH ₃ C ₄ H	CH ₃ C ₅ N	HC ₉ N	c-C ₆ H ₆
AlF	C ₂ H	l-C ₃ H	C ₄ H	l-H ₂ C ₄	CH ₂ CHCN	HC(O)OCH ₃	CH ₃ CH ₂ CN	(CH ₃) ₂ CO	CH ₃ C ₆ H	C ₂ H ₅ OCH ₃ ?
AlCl	C ₂ O	C ₃ N	C ₄ Si	C ₂ H ₄	CH ₃ C ₂ H	CH ₃ COOH	(CH ₃) ₂ O	(CH ₂ OH) ₂	C ₂ H ₅ OCHO	n-C ₃ H ₇ CN
C ₂	C ₂ S	C ₃ O	l-C ₃ H ₂	CH ₃ CN	HC ₅ N	C ₇ H	CH ₃ CH ₂ OH	CH ₃ CH ₂ CHO		
CH	CH ₂	C ₃ S	c-C ₃ H ₂	CH ₃ NC	CH ₃ CHO	C ₆ H ₂	HC ₇ N			
CH ⁺	HCN	C ₂ H ₂	H ₂ CCN	CH ₃ OH	CH ₃ NH ₂	CH ₂ OHCHO	C ₈ H			
CN	HCO	NH ₃	CH ₄	CH ₃ SH	c-C ₂ H ₄ O	l-HC ₆ H	CH ₃ C(O)NH ₂			
CO	HCO ⁺	HCCN	HC ₃ N	HC ₃ NH ⁺	H ₂ CCHOH	CH ₂ CHCHO (?)	C ₈ H ⁻			
CO ⁺	HCS ⁺	HCNH ⁺	HC ₂ NC	HC ₂ CHO	C ₆ H ⁻	CH ₂ CCHCN	C ₃ H ₆			
CP	HOC ⁺	HNCO	HCOOH	NH ₂ CHO		H ₂ NCH ₂ CN			2 atoms	3 atoms
SiC	H ₂ O	HNCS	H ₂ CNH	C ₅ N		CH ₃ CHNH			cont'd	cont'd
HCl	H ₂ S	HOCO ⁺	H ₂ C ₂ O	l-HC ₄ H					HF	H ₂ D ⁺
KCl	HNC	H ₂ CO	H ₂ NCN	l-HC ₄ N					HD	HD ²⁺
NH	HNO	H ₂ CN	HNC ₃	c-H ₂ C ₃ O					FeO ?	SiCN
NO	MgCN	H ₂ CS	SiH ₄	H ₂ CCNH (?)					O ₂	AlNC
NS	MgNC	H ₃ O ⁺	H ₂ COH ⁺	C ₅ N ⁻					CF ⁺	SiNC
NaCl	N ₂ H ⁺	c-SiC ₃	C ₄ H ⁻	HNCHCN					SiH ?	HCP
OH	N ₂ O	CH ₃	HC(O)CN						PO	CCP
PN	NaCN	C ₃ N ⁻	HNCNH						AlO	AlOH
SO	OCS	PH ₃ ?	CH ₃ O						OH ⁺	H ₂ O ⁺
SO ⁺	SO ₂	HCNO	NH ₄ ⁺						CN ⁻	H ₂ Cl ⁺
SiN	c-SiC ₂	HOCN							SH ⁺	KCN
SiO	CO ₂	HSCN							SH	FeCN
SiS	NH ₂	H ₂ O ₂							HCl ⁺	HO ₂
CS	H ₃ ⁺	C ₃ H ⁺ (?)							TiO ,	TiO ₂
cont'd	cont'd									

Information on many molecular species and their vibrational frequencies can be found in the NIST Vibrational and Electronic Energy database.¹³ Research has involved spectroscopic techniques such as microwave spectroscopy,¹⁴ photoelectron spectroscopy,¹⁵ and Fourier-transform infrared (FTIR) spectroscopy. Various methods of synthesizing clusters have been used including photolysis, laser ablation, and photon ionization.

Laser ablation, matrix trapping, and FTIR spectroscopy are central to the detection and characterization of Si-C molecules in the Molecular Physics Lab at Texas Christian University. The combination of FTIR measurements and *ab initio* theory has contributed to the first observations of vibrational fundamentals of ten species (shown in Figure 1.1): SiC₂, SiC₄, Si₂C,¹⁶ Si₂C₂,¹⁷ and Si₃C,¹⁸ SiC₃Si,¹⁹ and Si₃C₂,²⁰ SiC₄Si,²¹ SiC₉,²² and SiC₇.²³ In the past, many molecules were made using high-temperature evaporation from Knudsen cells, although it was found difficult to create molecules of more than four atoms. In 1999 and 2000, Ding *et al.* synthesized SiC₉, and SiC₇ using Nd-YAG laser evaporation of silicon-carbon rods.^{22, 23}

While gas phase studies of molecules are more ideal than matrix studies, (because, in gas phase, the molecule is not perturbed by a matrix), they are generally more difficult to conduct for several reasons. First, in the gas phase, the molecules are free to rotate and rotational spectra are more difficult to analyze than infrared vibrational spectra recorded at very low temperatures (~10 K). Second, in the case of microwave spectroscopy, detecting a pure rotational spectrum necessitates a permanent dipole moment. However, in infrared spectroscopy, we can observe the bending, and asymmetric stretches of a molecule without a permanent dipole moment. Third, synthesizing molecules is difficult because the yield in the gas phase is low, while in matrix trapping, molecules are held in one place and we can build upon already made concentrations of

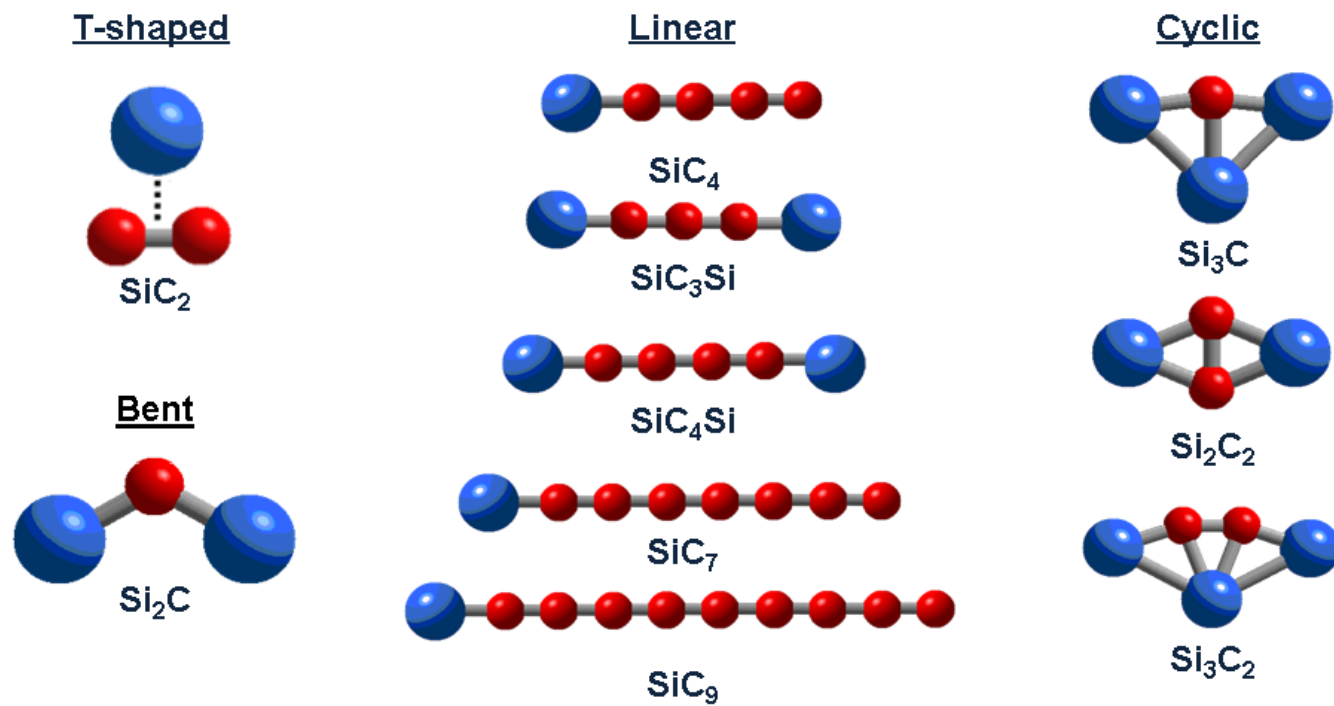


Figure 1.1. Previously identified Si_nC_m by researchers in the Texas Christian University (TCU) Molecular Physics lab (MPL).

molecules. A fourth reason is that detecting gas phase molecules is usually done by diode laser spectroscopy, which is complicated by the very narrow frequency tuning ranges for diodes; this makes looking for new species in a broad spectral survey very time consuming. Matrix measurements are very useful because they help experimentalists to narrow the frequency range where a molecule's gas phase frequencies are expected to be found. The advantage of matrix measurements for new species is that they are easier to acquire than gas phase measurements, and are often within a few percent of gas phase values. In addition, a comprehensive study by Jacox²⁴ has shown that matrix measurements are much more useful in predicting gas phase values than theoretical predictions (see Figure 1.2):

“The neon- and argon- matrix observations deviate from the gas phase band centers by less than one fifth as much as do any of the calculations included in the comparison, and the spread of the deviations is less than 1%.”

The previously discussed matrix identifications have provided a starting point for subsequent Si-C investigations. The observations of the $\nu_3(\sigma)$ fundamental of SiC₄ and of $\nu_3(\sigma_u)$ fundamental of SiC₃Si have helped experimentalists make gas phase measurements using high-resolution diode spectroscopy.^{25, 26} McCarthy *et al.* found the rotational spectra of five linear SiC_{*n*} (*n* = 3, 5–8) clusters using Fourier transform microwave (FTMW) spectroscopy.¹⁴ The clusters were made using a gas discharge through silane and diacetylene and by the evaporation of graphite and silicon. They reported rotational spectra, centrifugal distortion constants, spin-spin constants and spin-rotation coupling constants. A few years later, McCarthy *et al.* reported having found more than twenty silicon-bearing molecules.²⁷ Pellarin *et al.* studied Si_{*n*}C_{*m*} clusters made from laser vaporization using mass spectroscopy.²⁸

Taking advantage of the experimental data that was available, theorists have performed many systematic studies, mainly using density functional theory (DFT). Hunsicker and Jones²⁹ studied anionic and neutral Si_nC_m clusters containing up to eight atoms, and found that carbon-rich clusters tended to form chain-like structures and silicon-rich clusters tend to form 3-dimensional geometries. Bertolus *et al.* studied Si_nC_m ($m+n = 3$ or 6) and predicted the correct ground states, energetic orders, and vibrational frequencies to within 3% of the experimental values.³⁰ Botschwina and Oswald studied SiC_3 and SiC_5 to predict equilibrium dipole moments and various spectroscopic constants.³¹ Jiang *et al.* found that SiC_{m-1} ($m = 3-9$) form linear structures, SiC_{m-1} ($m = 10-16$) form cyclic structures, and $\text{Si}_2\text{C}_{m-2}$ ($m = 4-16$) form linear structures, except for Si_2C_{12} .³² Deng *et al.* studied thermodynamic properties and determined the structures and vibrational frequencies of Si_mC_n ($3 \leq n+m \leq 6$) in their ground electronic states.³³

1.3 FOCUS OF THE PRESENT RESEARCH

Si-C clusters are currently the subject of ongoing research by the TCU Molecular Physics Laboratory because of their potential applications to astrophysics and the study of Group IV molecules. In the present work, the synthesis and observation of vibrational fundamentals of silicon-carbon species, SiC_5 and SiC_5Si will be discussed.

The only previous experimental work on SiC_5 has been done by McCarthy *et al.*, who found its rotational spectrum.¹⁴ Previous theoretical works have predicted the lowest electronic structure of SiC_5 to be triplet linear.²⁹⁻³³ Many predictions for the properties of SiC_5 have been made. Of these predictions, the three most intense vibrational modes of SiC_5 are shown in Table 1.2.

In regards to SiC₅Si, two major studies have been previously reported. In simulating the vaporization process of meteorites in Titan's atmosphere, Kaiser *et al.* synthesized the molecule and detected it using mass spectroscopy. They measured its photoionization energy to be 8.5 ± 0.1 eV and did not comment on the ground state structure.³⁴ The only previous theoretical work was done by Jiang *et al.*, using DFT - B3LYP/6-311G*, (that is Becke 88 three-parameter exchange and Lee-Yang-Parr correlation functional) they calculated the most intense mode of linear SiC₅Si to be $\nu_4(\sigma_u) = 2144 \text{ cm}^{-1}$.³⁵

The experimental techniques used to produce and identify these two molecules will be discussed in Chapter II. And following discussions will explain these investigations in more detail, ending with possible ideas for future research.

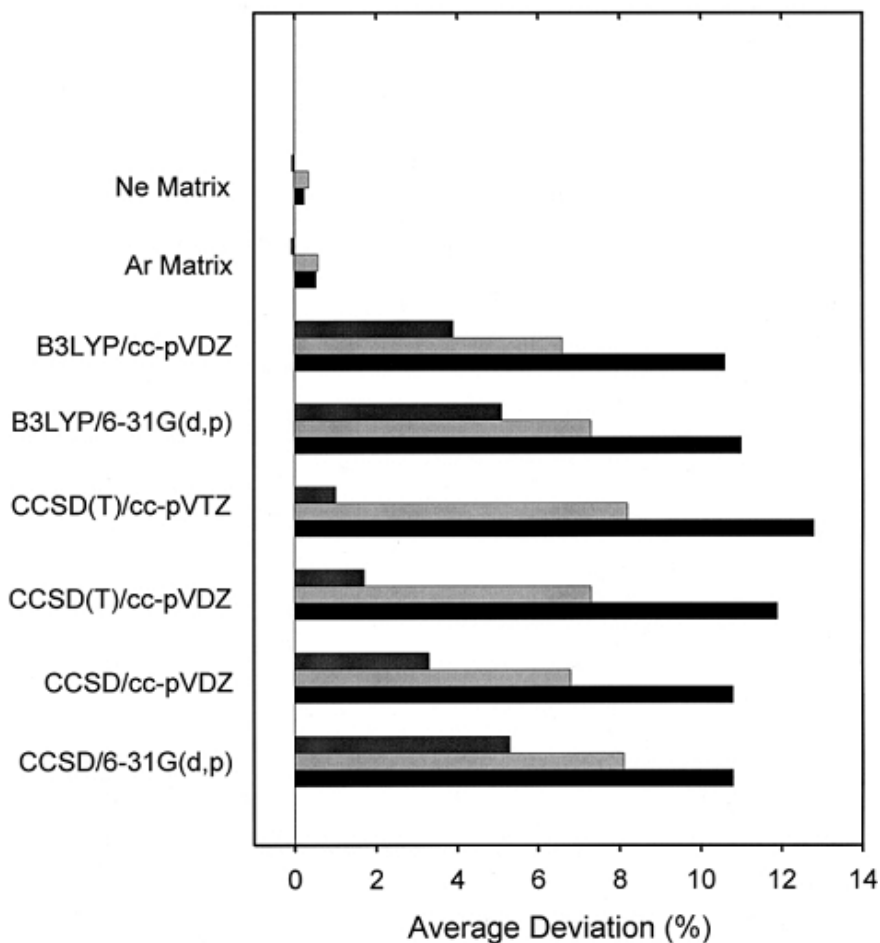


Figure 1.2 The average deviations of neon- and argon-matrix frequencies and of unrestricted calculations of vibrational fundamentals of free radicals from observed gas-phase values. In each group, top = numerical average, middle = absolute average, and bottom = standard deviation. This graph was reported by Jacox in Ref. 24.

Table 1.2 Three Predicted Vibrational Fundamentals of SiC₅. Please refer to the glossary for the definitions of acronyms.

Reference	Level of Calculation	Three Most Intense Predicted Vibrational Fundamentals of SiC ₅ (cm ⁻¹)
30	DFT – LSDA/VWN	959.7, 1966.5, 2140.2
33	DFT – B3PW91/6-31G(d)	928.6, 1889.2, 2041.9
36	MP2	977, 1965, 2091

CHAPTER II

EXPERIMENTAL PROCEDURES

2.1 FOURIER TRANSFORM INFRARED SPECTROSCOPY

In the present research, molecules are detected via vibrational spectra that are measured using FTIR absorption spectroscopy. Many properties of a molecule, such as the masses of participating atoms, atomic composition and molecular structure, affect its vibrational frequencies. In general, N -atom molecules have $3N-6$ vibrational modes ($3N-5$ if a linear molecule). Vibrational modes, which have an oscillating dipole moment and quantum mechanically allowed transitions, absorb infrared radiation and are described as “infrared active.” The bands in infrared spectra belong to different molecular vibrations. Each molecule has a unique vibrational spectrum often referred to as its “infrared signature.”

In the present work, vibrational spectra are detected using an FTIR spectrometer (BOMEM DA 3.16) that is built around a Michelson interferometer as shown in Figure 2.1. FTIR absorption spectra are recorded from 500 to 5000 cm^{-1} at a resolution of 0.2 cm^{-1} . The beam splitter in the spectrometer is KBr, which has a range of 500 to 6000 cm^{-1} . The detector is a HgCdTe (MCT) detector with range 150 to 12000 cm^{-1} and maximum sensitivity in the 2000 cm^{-1} region.

2.2 SAMPLE PREPARATION: MATRIX TRAPPING AND LASER ABLATION

The process of molecular synthesis has three main parts: rod preparation, laser ablation, and matrix trapping. Molecules are made by vaporizing the surface of a rod compressed from powdered mixtures, entraining the vapor in an excess of Ar gas (molecule to Ar ratio is $\sim 1:100$),

and condensing it on a cold, gold mirror held at ~ 20 K. In order to produce a detectable number of molecules, deposition may be for 2–3 hours. After deposition of the matrix sample, which contains molecules trapped in Ar on the mirror, annealing is often done to sharpen spectra or to encourage diffusion and reaction of the molecules in the matrix. During annealing, the gold mirror is heated by ~ 3 – 10 K, maintained at this temperature for 5–60 minutes, and then quenched down to 20 K. Warming the mirror can cause surface molecules and surface atoms to evaporate, molecules within the matrix to diffuse and react, and other molecules remain unchanged. Diffusion and reaction can be used to create new molecular species. When molecules are trapped at multiple trapping sites, annealing encourages diffusion to the lowest energy site and consequently simplifies the spectrum.

Figure 2.3 shows a top view of the experimental setup. Radiation (1064 nm) from a Nd-YAG laser (Spectra Physics, Quanta Ray models DHS-2, GCR-11, and INDI) is directed toward the sample chamber, passing through a quartz window to the silicon and carbon rods. Once the molecular vapor is condensed with Ar on the gold mirror, it is rotated to face the spectrometer for data acquisition. An absorption spectrum is recorded by monitoring radiation that is emitted from the Globar source, passes twice through the condensed sample on being reflected from the gold mirror substrate, and then absorbed by the detector, as shown in Figure 2.1. The sample chamber and spectrometer are held, respectively, at vacuum pressures of $\sim 10^{-8}$ Torr (to prevent the formation of contaminants in the sample) and $\sim 10^{-3}$ (to reduce the presence of H_2O and CO_2). In addition, they are separated by a CsI window, which is transparent in the mid-infrared (~ 500 – 7000 cm^{-1}).

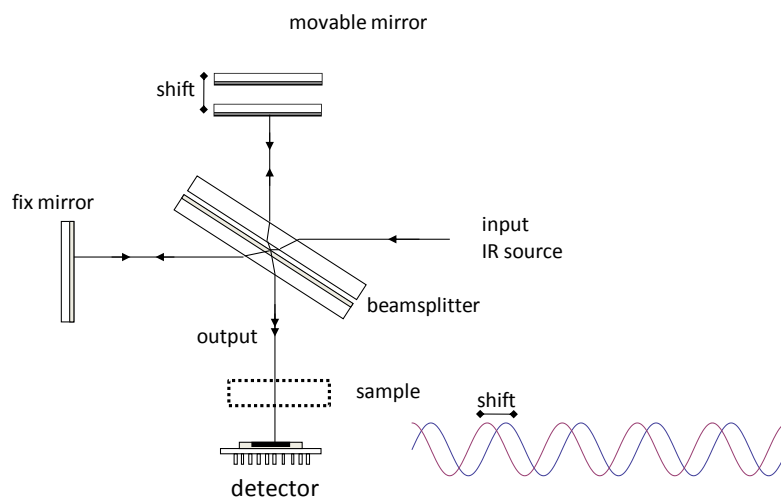


Figure 2.1 Diagram of the Michelson interferometer.

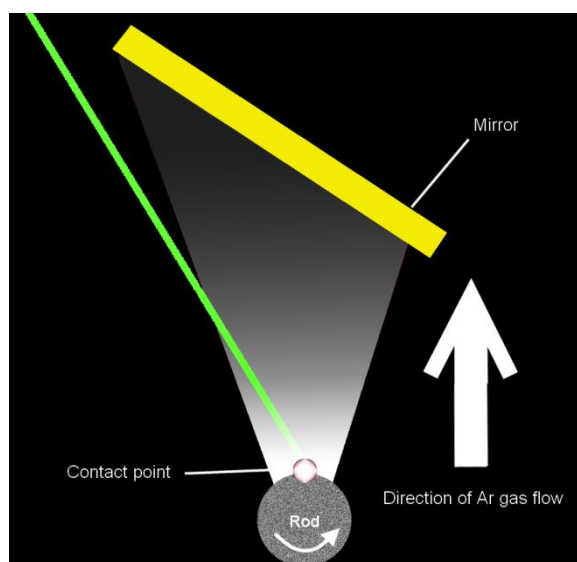


Figure 2.2 Top down view showing laser ablation of a sample rod, the resulting vapor, and the gold mirror on which molecules are trapped. The rod is continually rotated and translated vertically during ablation.

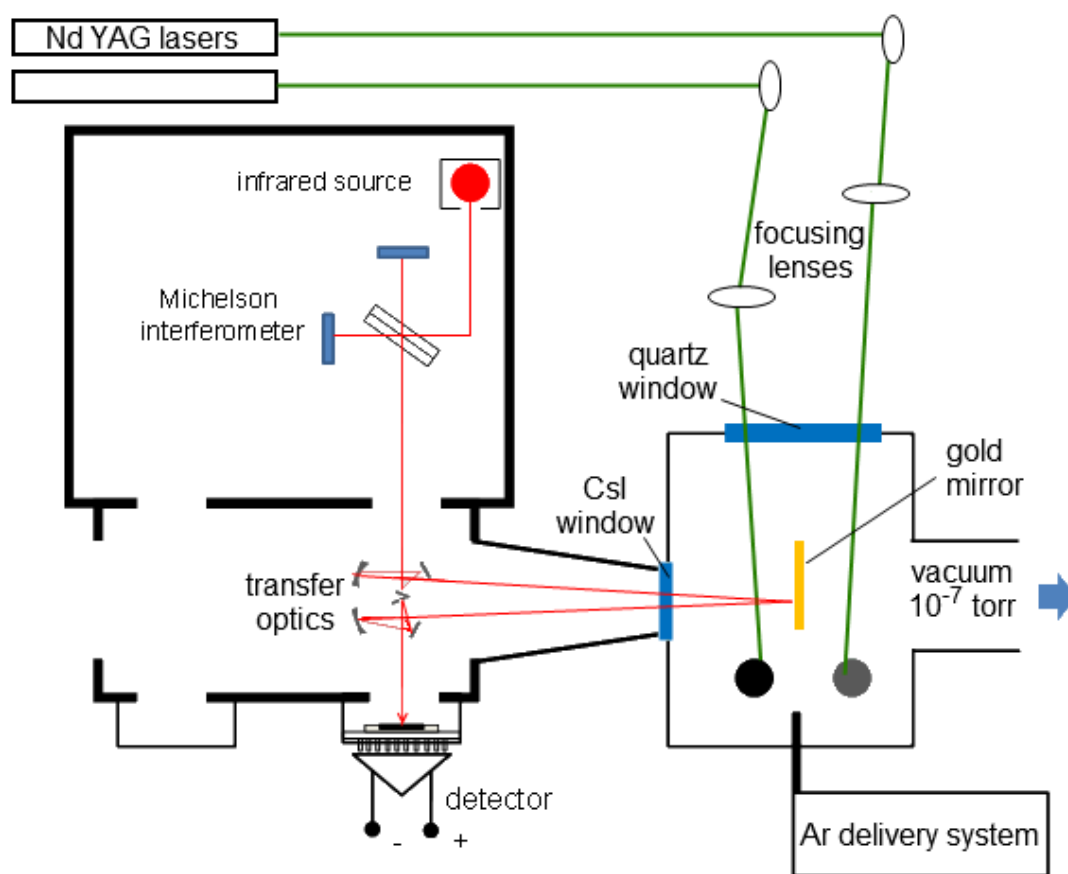


Figure 2.3 Top view of experimental setup. Not to scale.

2.2.1. Rod Preparation

In order to observe isotopic frequency shifts (to be discussed in further detail in Section 2.3), rods are prepared with specific amounts of the carbon-13 (Alfa Aesar, 99.9995% purity) and carbon-12 isotopes (Isotec 99.3% purity respectively). If substitution at each site in the molecule is random and a graphite rod with 10% ^{13}C (by mol) enrichment is ablated, then the probability of yielding a C_n molecule with a single ^{13}C substitution is $10\% \cdot (90\%)^{n-1}$. While the probability of yielding a C_n molecule with no ^{13}C substitution is $(90\%)^n$. Then the relative intensity of the singly-substituted $^{13}\text{C}_n$ molecule with respect to the $^{12}\text{C}_n$ molecule is $\frac{10\% (90\%)^{n-1}}{(90\%)^n} = 11\%$. Therefore, when analyzing the integrated intensities of the isotopomer bands, an integrated intensity of 11% for an isotopomer band relative to the fundamental band implies that the band is associated with a single ^{13}C substitution. Similarly, a ~22% integrated intensity implies that there is a pair of symmetrically equivalent carbon atoms. This information helps in analyzing isotopic shift bands and identifying the carrier responsible for the vibrational fundamental, the details of which are explained in a later section. In general, a rod is formed by pressing powder using a SPEX (nominal 30-ton) press at 4.5×10^5 kPa.

A rod's density affects its evaporation characteristics and thus the species produced. Rods are prepared in two ways. In the so-called "soft rod" technique, the powders are pressed at 4.5×10^5 kPa, but not sintered. Rods produced in this way increase the production of small molecules (≤ 4 atoms). The powders may be pre-baked to reduce contaminants such as CO_2 and H_2O . In the second method, the rod is sintered at temperatures below the melting point of the metal powders under vacuum in an oven. Sintering increases densification so that when the rod is laser ablated the production of larger chain molecules (> 4 atoms) is favored over that of smaller molecules. In cases where the ratio of Si to C is high, *e.g.* 20% Si / 70% ^{12}C , caution

must be exercised such that temperature gradients are not too large (*e.g.* an increase or decrease of 40°C in a minute is too large) and cause fracturing of the rod due to different thermal expansion properties of Si and C powder.

2.2.2. *Laser Ablation*

Laser ablation is the vaporization of the surface of the sample rod with a laser beam to form atoms and molecules as shown in Figure 2.2. The power of the laser beam per unit area of the sample surface is a major factor in molecule production. Using a low power (< 1W) and tight laser focus makes the laser contact area < 3 mm in diameter, yielding mostly C₂ and C₃ molecules. Factors, such as high laser powers (> 2 W) and a loose focus, which has a contact area ~3 – 6 mm, yield mostly long chain molecules (*e.g.* C₆, C₉, and C₁₂).

2.2.3. *Matrix Trapping*

Inside the vapor resulting from laser ablation, chemical reactions occur and produce new species. It has been observed that at the contact point between the laser beam and the rod, a bright color is given off, or “contact color” as it will be referred to from now on, correlates with various laser experimental conditions. A white colored plume usually indicates sputtering in which chunks of graphite are ablated from the rod rather than molecules or atoms. This is confirmed by a rapid drop in the signal-to-noise ratio of absorbance spectra. A violet color is characteristic of a tight focus and low laser power. A yellowish color is generally observed when a loose focus and high power is used. In the case of the yellow color, it has been found that the signal does not drop dramatically, which implies that atoms and molecules are being vaporized with very little sputtering. The ablation products are then swept up by a beam of Ar gas, and condensed on a gold mirror at ~15 K (Figure 2.2). (At atmospheric pressure, Ar is a solid below 80 K.) When the vapor condenses on the cold mirror, the molecules are trapped in

micro-crystallites. These molecules are generally trapped in their ground electronic states and cannot rotate, which greatly simplifies the infrared spectrum.

2.3 ISOTOPIC SHIFT PATTERNS

To identify a novel Si-C molecule, we analyze unidentified Si-C bands and produce isotopomers of the molecule by enriching the starting material with a heavier isotope, such as carbon-13. The isotopomers will have vibrational frequencies that are shifted from the vibrational fundamental. The frequency differences between the isotopomers bands and the fundamental band, called “isotopic shifts”, are unique to a particular isomer.

From the isotopic shift spectra, we can find important information regarding the molecule’s structure. If all carbon atoms in the molecule are distinguishable, then there would be an equal probability of producing all possible single ^{13}C isotopomers. For example, linear SiC_5 would have five distinct single ^{13}C isotopomers, one for substitution at each of the inequivalent carbon atom sites (Figure 2.4). Each isotopomer would have the same probability of being made as the other singly substituted ^{13}C isotopomers, and the corresponding infrared bands would all have the same intensities. If not all carbon atoms were distinguishable, the isotopic shift spectrum would be different. For example, a linear C_6 molecule results in three isotopic shifts corresponding to three pairs of symmetrically equivalent carbons (Figure 2.5). Each isotopomer band’s intensity is approximately 20% of the fundamental band. Thus, from the isotopic spectra, it is possible to deduce the structure and formula of the molecule.

A similar analysis can be done with stable Si-isotopes, ^{29}Si , and ^{30}Si . However, instead of enriching rods with ^{29}Si and ^{30}Si , we rely on their natural abundances, 4.67% and 3.1%,

respectively, to produce Si-isotopomers. This means that the isotopic shift bands would have intensities of approximately 5% and 3% compared to the intensity of the fundamental band.

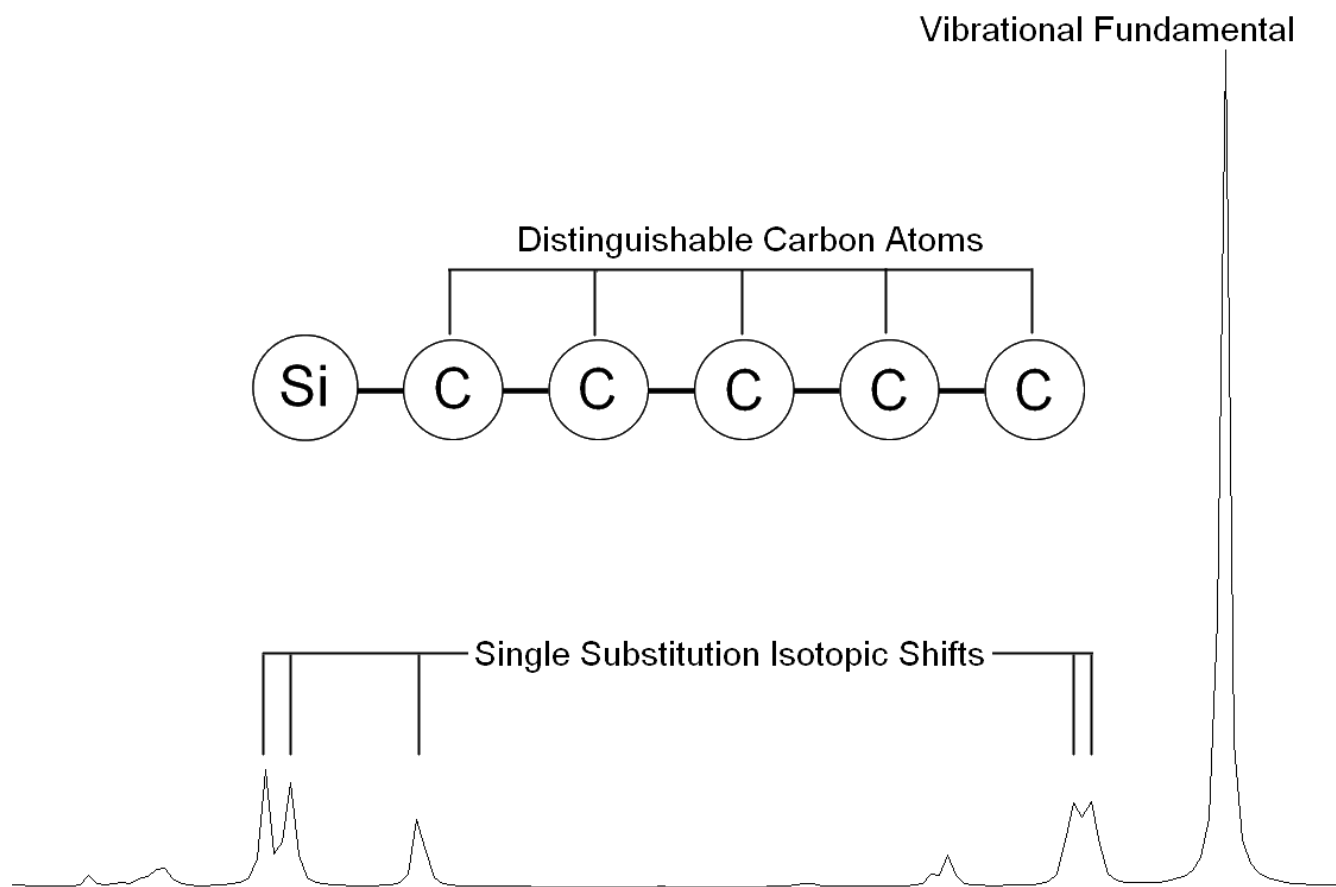


Figure 2.4 Simulation of the 10% ¹³C isotopic shift pattern of a vibrational mode of SiC₅.

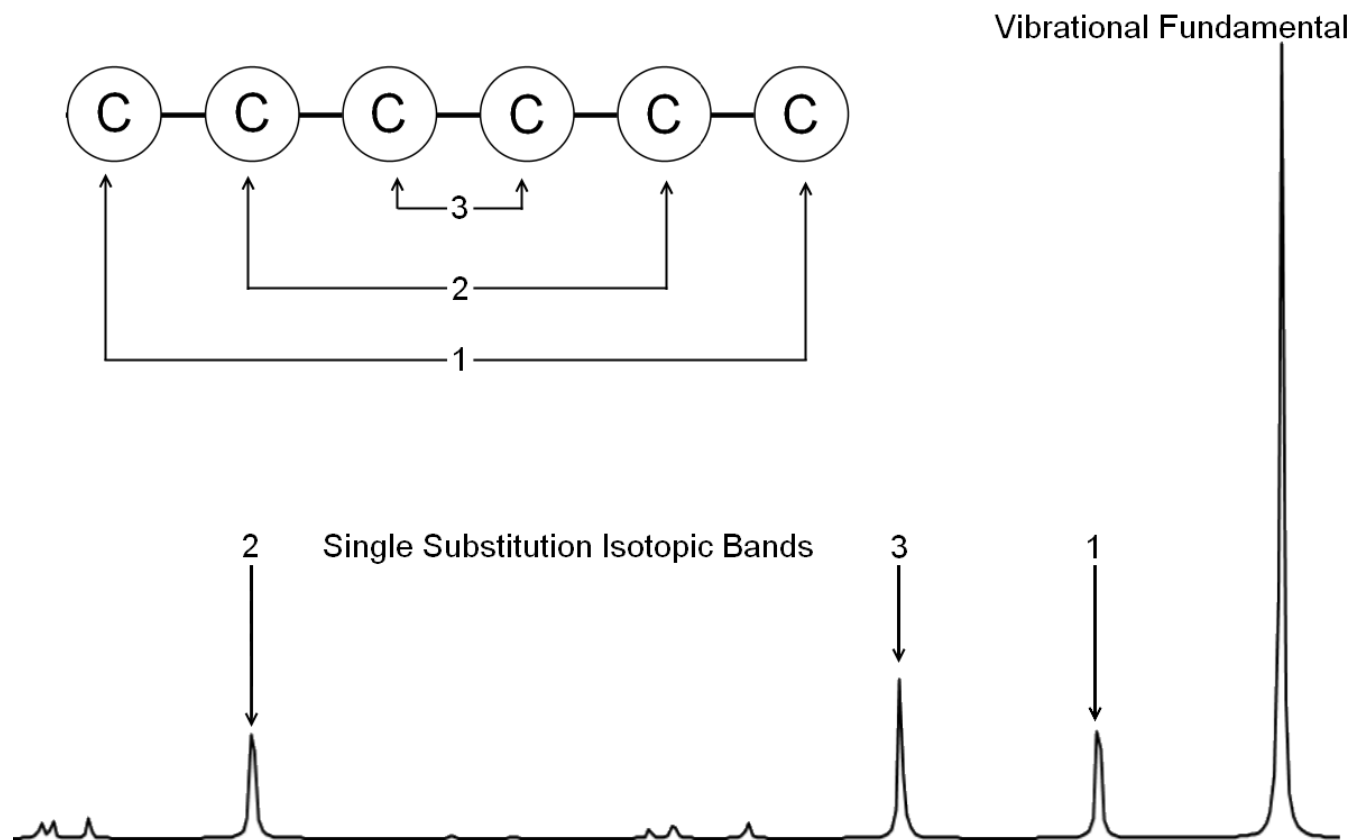


Figure 2.5 Simulation of the 10% ^{13}C isotopic shift pattern of a vibrational mode of C_6 . The numbers 1, 2, and 3 identify the pairs of symmetrically equivalent carbon atoms responsible for the shifts.

CHAPTER III
FTIR ISOTOPIC STUDY OF SiC₅
IDENTIFICATION OF THE ν_4 MODE

3.1 INTRODUCTION

A great deal of research has been done on SiC_n species, because of the application to the study of Group IV molecules and the potential application of molecular species in circumstellar shells and the interstellar medium. It has been noted that other SiC_n molecules consisting of a single silicon atom terminally bonded to a carbon chain are particularly good candidates for detection by radio astronomy in circumstellar shells³⁷ because of their predicted high polarity. So far rhomboidal SiC₃ (Ref. ³⁸) and linear SiC₄ (Ref. ³⁹) have been observed in the carbon star IRC +10216. In the case of linear silicon carbide molecules, theoretical and experimental laboratory investigations have been reported for SiC_n, n=3-9.

The linear isomer of SiC₃ is the simplest mono-silicon carbon chain (SiC_n, where $n \geq 3$). In a study of the photoelectron spectroscopy of the SiC₃⁻ anion Davico *et al.*⁴⁰ identified C-C stretching modes at 1980 ± 20 and 1320 ± 20 cm⁻¹ for the neutral in the $^3\Sigma^-$ state, consistent with theoretical predictions by Rintelman and Gordon.⁴¹ The rotational spectra for two C_{2v} ring isomers of SiC₃ with transannular C-C (Ref. 42) and Si-C (Ref. 43) bonds, and a linear triplet³⁷ were observed in a gas discharge through a mixture of silane and diacetylene by Thaddeus and collaborators using Fourier transform microwave spectroscopy (FTMW). The most advanced calculations using multi-reference, second-order perturbation theory (MRPT2), indicate that the isomer of SiC₃ with singlet rhombic structure and transannular C-C bond should be lowest in

energy.⁴¹ The linear triplet isomer is predicted to lie only 2.2 kcal/mol higher and the singlet rhombic isomer with transannular Si-C bond 4.7 kcal/mol above the minimum.

The vibrational spectrum of linear SiC₄ was first reported by Withey *et al.*⁴⁴ in the products from the photolysis of silane and 1,3-butadiene trapped in solid Ar. The ν_1 C-C stretching fundamental was identified on the basis of agreement between measured ¹³C isotopic shifts and second-order Møller-Plesset [MP2/6-311G(d)] predictions.⁴⁵ Subsequently the band was measured in the gas phase at high resolution using diode laser spectroscopy.⁴⁶ Gordon *et al.*⁴⁷ reported a detailed investigation of the structure and molecular constants of both SiC₄ and SiC₆. Measurements of the rotational spectra with FTMW spectroscopy using ¹³C isotopic substitution were made in combination with extensive *ab initio* calculations, including coupled cluster, with single, double and triple excitations (CCSD(T)). This work and other theoretical studies^{48,49} confirm that the linear isomer is the most stable structure for both SiC₄ and SiC₆. At this point no observation of the vibrational spectrum has been reported for SiC₆; this is likely caused by the molecule's most intense vibrational mode lying within the crowded C-C stretching region.

Of the remaining linear SiC_n chains with $n=5$, and 7-9, the $\nu_1(\sigma)$ fundamental of SiC₇ was first observed in the TCU Molecular Physics Laboratory at 2100.8 cm⁻¹ (Ref. 50) and the $\nu_4(\sigma)$ of SiC₉ at 1935.8 cm⁻¹ (Ref. 51) in the products, from the dual laser evaporation of silicon and carbon rods or a fabricated silicon/carbon rod, that were trapped in solid Ar. Identifications were made by comparing measured ¹³C isotopic shifts with the predictions of DFT calculations at the B3LYP/cc-pVDZ level. In addition to the experimental conclusion that SiC₉ is linear, two subsequent studies on the basis of DFT calculations have suggested the possibility that SiC₉ may have one or more ring structures.^{52,53}

Efforts to detect the vibrational spectra of SiC₅ and SiC₈, using a similar approach that which produced SiC₇ and SiC₉, have been unsuccessful, until the work on SiC₅ that is reported here. Using FTMW spectroscopy, McCarthy *et al.*³⁷ have identified with the assistance of *ab initio* calculations by Rittby⁵⁴ the rotational spectra of the linear SiC_n (*n*=3, 5-8) molecules formed in a glow discharge through silane and acetylene. The electronic ground state was found to be $X^1\Sigma^+$ for even *n* and $X^3\Sigma^-$ for odd.

This chapter presents the first observation of the vibrational spectrum of SiC₅. As noted earlier, McCarthy *et al.* have previously reported its rotational spectrum and confirmed its linear structure.⁴³ Previous theoretical work has predicted the lowest electronic structure of SiC₅ to be triplet linear.^{44,55-57}

3.2 EXPERIMENT

SiC₅ was produced by laser ablation of a sintered carbon rod with 5% (by mol) Si content. The evaporation was carried out using an Nd:YAG laser (Spectra Physics) operating at 1064 nm in the pulsed mode. The evaporated species were condensed in solid Ar (Matheson, 99.9995% purity) on a gold surfaced mirror cooled to ~20 K by a closed cycle refrigeration system (ARS, Displex). The mirror was enclosed in a vacuum chamber maintained at a pressure of ~10⁻⁸ Torr.

Experimental parameters such as laser focus, laser power, and Ar flow were adjusted to favor the production of SiC₅. For the laser ablation of the sintered Si/C rod, a laser beam with a power of 2.5 W with moderately loose focus on an area of ~2.5 mm² was used. During deposition, the Ar flow rate was adjusted by opening a needle valve until the sample chamber pressure increased from ~10⁻⁸ to ~10⁻⁵ Torr. Typically, matrix samples in the experiments discussed here were deposited for 90 min. In order to unambiguously determine the molecular structure and identify vibrational fundamentals, it is crucial to measure isotopic shifts. For this

purpose, Si/C rods were fabricated with a mixture of ^{12}C (Alfa Aesar, 99.9995% purity), and ^{13}C (Isotec, 99.3% purity) in a percent molar ratio of 5% Si: 85% ^{12}C :10% ^{13}C .

Fourier transform infrared (FTIR) absorption spectra of the products trapped in Ar matrices were recorded over the range of $500 - 3500 \text{ cm}^{-1}$ at a resolution of 0.2 cm^{-1} using a Bomem DA3.16 Fourier transform spectrometer equipped with liquid nitrogen cooled Hg-Cd-Te detector and KBr beamsplitter. Details of the optical system have been reported previously.⁵⁸

3.3 RESULTS AND ANALYSIS

Potential candidates for Si_nC_m absorptions in the $500 - 3500 \text{ cm}^{-1}$ range were identified by comparing spectra produced by the ablation of a sintered, mixed Si/C rod to spectra produced by pure graphite ablation. Many candidates were found, and in the 900 to 950 cm^{-1} region that is relatively clear of crowding bands, a strong, unidentified absorption attributable to a Si_nC_m species was observed at 936.9 cm^{-1} as shown in Figure 3.1(b).

Comparison of spectra produced by the ablation of a sintered Si/C rod to that produced from a graphite rod (Figure 3.1) indicates that the unidentified 936.9 cm^{-1} absorption probably belongs to a Si_nC_m species. The nearby 922.8 cm^{-1} absorption, which appears only on graphite rod ablation, is probably an as-yet-unidentified C_n band. The two weaker bands at 935.2 and 933.5 cm^{-1} , could be either modes of other Si_nC_m species, or more likely, Si isotopic shift bands belonging to the 936.9 cm^{-1} absorption. Silicon-29 and 30 isotopes occur in relative natural abundance of 4.7 and 3.1%, respectively. If the two weaker bands are Si isotopic shifts, their intensity ratios with respect to the fundamental should be 5.1 and 3.4%, respectively, which are very close to those observed. This result suggests that the carrier of the 936.9 cm^{-1} band probably has at least one Si atom.

To determine the number of carbon atoms in the molecule, experiments with 10% ^{13}C enrichment were carried out to produce ^{13}C -isotopic shifts predominantly for single ^{13}C -substituted isotopomers. Figure 3.2(a) shows five distinct, new bands observed to the low frequency side of the 936.9 cm^{-1} band and, labeled D thru H, that are candidates for single ^{13}C isotopomers. Other weaker absorptions are possible double ^{13}C -substituted isotopomers. The intensities of the five strong bands are consistently $\sim 10\%$ of the fundamental and remain so even after annealing at 30 K for 18 min and at 33 K for 30 min. This behavior indicates that they are all single ^{13}C -isotopic shifts of the 936.9 cm^{-1} fundamental and, consequently, that the carrier contains at least five inequivalent carbon atoms. The simplest molecule likely to produce the observed isotopic spectrum is linear SiC_5 , with a chain of five carbon atoms and a terminal Si atom.

Comparison of the observed ^{13}C isotopic shift spectrum with DFT simulated isotopic spectra provides the critical test for confirming the tentative identification of SiC_5 and determining the isomer and vibrational fundamental. Linear SiC_5 can have a singlet or triplet spin multiplicity; however, a DFT calculation with the B3LYP (Becke three parameter exchange and Lee-Yang-Parr correlation)^{59,60,61} functional and cc-pVDZ basis in the GAUSSIAN 03 suite of programs shows that the energy of the linear singlet form is ~ 12 kcal/mol higher than the triplet linear. Table 3.1 shows the calculated frequencies of the vibrational fundamentals for the $^3\Sigma^-$ state and Table 3.2 shows the corresponding calculated bond lengths. Comparison with the observed 936.9 cm^{-1} frequency suggests that it is a likely candidate for the $\nu_4(\sigma)$ fundamental of SiC_5 predicted at 960 cm^{-1} .

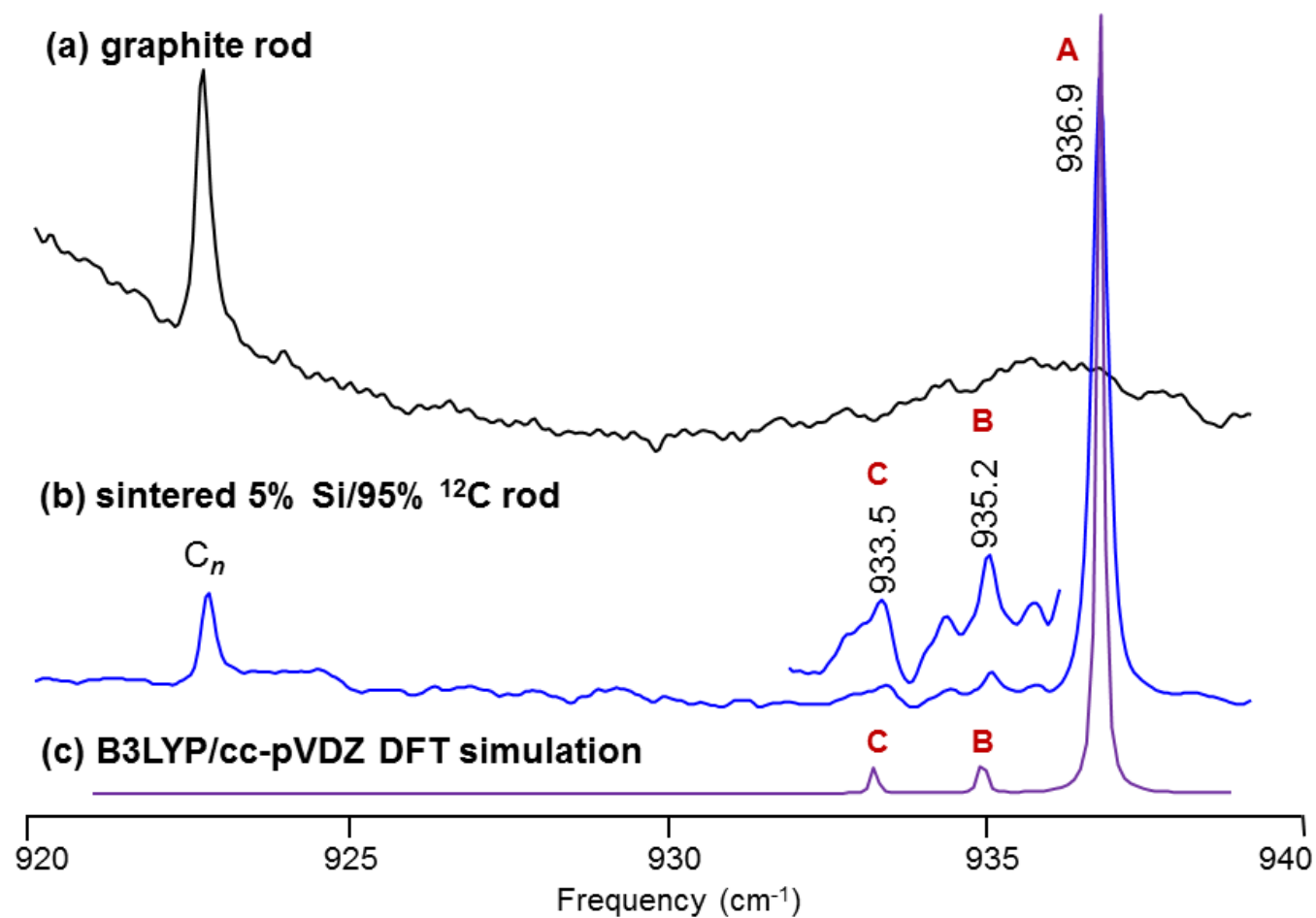


Figure 3.1 Comparison of the FTIR spectra produced by the ablation of (a) graphite rod, (b) a sintered, mixed 5% Si / 95% C rod, (c) a DFT simulation at the B3LYP/cc-pVDZ level of the $^{29,30}\text{Si}$ -isotopic shifts for the $\nu_4(\sigma)$ mode of linear, triplet SiC_5 . Isotopomer frequencies in the spectrum in (b, c) are labeled according to the list in Table 3.3.

Table 3.1. DFT-B3LYP/cc-pVDZ predicted vibrational modes, frequencies (cm^{-1}), and infrared intensities (km/mol) for linear, triplet ($^3\Sigma$) SiC_5 .

Vibrational mode	Frequency (cm^{-1})	Infrared intensity (km/mol)
$\nu_1(\sigma)$	2116	315
$\nu_2(\sigma)$	1966	491
$\nu_3(\sigma)$	1547	12
$\nu_4(\sigma)$	960	27
$\nu_5(\sigma)$	495	14
$\nu_6(\pi)$	648	2
$\nu_7(\pi)$	413	0
$\nu_8(\pi)$	212	20
$\nu_9(\pi)$	85	2

Table 3.2. DFT-B3LYP/cc-pVDZ predicted bond lengths for linear, triplet ($^3\Sigma$) SiC_5 .

Bond	Predicted Bond Length (\AA)
Si - C1	1.73938
C1 - C2	1.28810
C2 - C3	1.29135
C3 - C4	1.29649
C4 - C5	1.30462

The ^{13}C isotopic shift spectrum observed for the 936.9 cm^{-1} absorption and the DFT simulated spectrum are compared in Figure 3.2. The observed spectrum resulting from the ablation of a sintered rod containing a mixture of 5% Si/ 10% ^{13}C /85% ^{12}C appears in Figure 3.2(a) and the DFT-simulated ^{13}C isotopic shift spectrum for the $\nu_4(\sigma)$ mode of linear SiC_5 , in Figure 3.2(b). Visually, the simulated and observed isotopic shift patterns appear very similar and Table 3.3 shows that the discrepancies between the measured and DFT predicted ^{13}C shifts are 1.4 cm^{-1} or less. Similarly, the DFT simulation, for the $^{29,30}\text{Si}$ -isotopic shifts, shown in Figure 3.1(c) and labeled B and C, respectively, is very similar to the observed shifts in Figure 3.1(b). As shown in Table 3.3, the discrepancies between the measured and calculated $^{29,30}\text{Si}$ shift bands are 0.2 cm^{-1} or less. On the basis of the close agreement between the measured and DFT-predicted $^{29,30}\text{Si}$, and ^{13}C -isotopic shifts the absorption at 936.9 cm^{-1} can therefore be confidently assigned to the $\nu_4(\sigma)$ fundamental of linear SiC_5 . As shown in Table 3.3, the DFT-B3LYP/cc-pVDZ calculation predicts that six of the vibrational fundamentals of linear SiC_5 are potentially in the $500 - 3500\text{ cm}^{-1}$ range of our measured spectra although $\nu_4(\sigma)$ is relatively very weak. The ν_1 and ν_2 fundamentals are predicted to be, respectively, ~ 12 and ~ 18 times more intense than the observed ν_4 fundamental. However, after performing many experiments to optimize the intensity of the ν_4 fundamental no candidates for the other fundamentals were found, because these lie in the crowded C-C stretching region and many bands' isotopic shift patterns overlap, as shown in Figure 3.3. The absorbance intensities of the strongest C-C stretching bands (such as SiC_9 , C_{11} , C_6 , etc.) are so strong that, even if ν_1 and ν_2 absorptions are ~ 12 or 18 times the intensity of ν_4 , as theory predicts, their isotopic shift patterns are dwarfed and overlapped.

3.4 CONCLUSION

This is the first report of the vibrational spectrum of linear SiC₅. Although DFT-B3LYP/cc-pVDZ calculations predict the ν_1 , ν_2 and ν_4 modes to be most intense, our experimental data have enabled only the identification of the ν_4 mode. The agreement between the measured ¹³C-isotopic shifts and the predictions of DFT calculations confirms the assignment of a band at $936.9 \pm 0.2 \text{ cm}^{-1}$ to the $\nu_4(\sigma)$ mode, an asymmetric stretch of linear SiC₅, trapped in solid Ar.

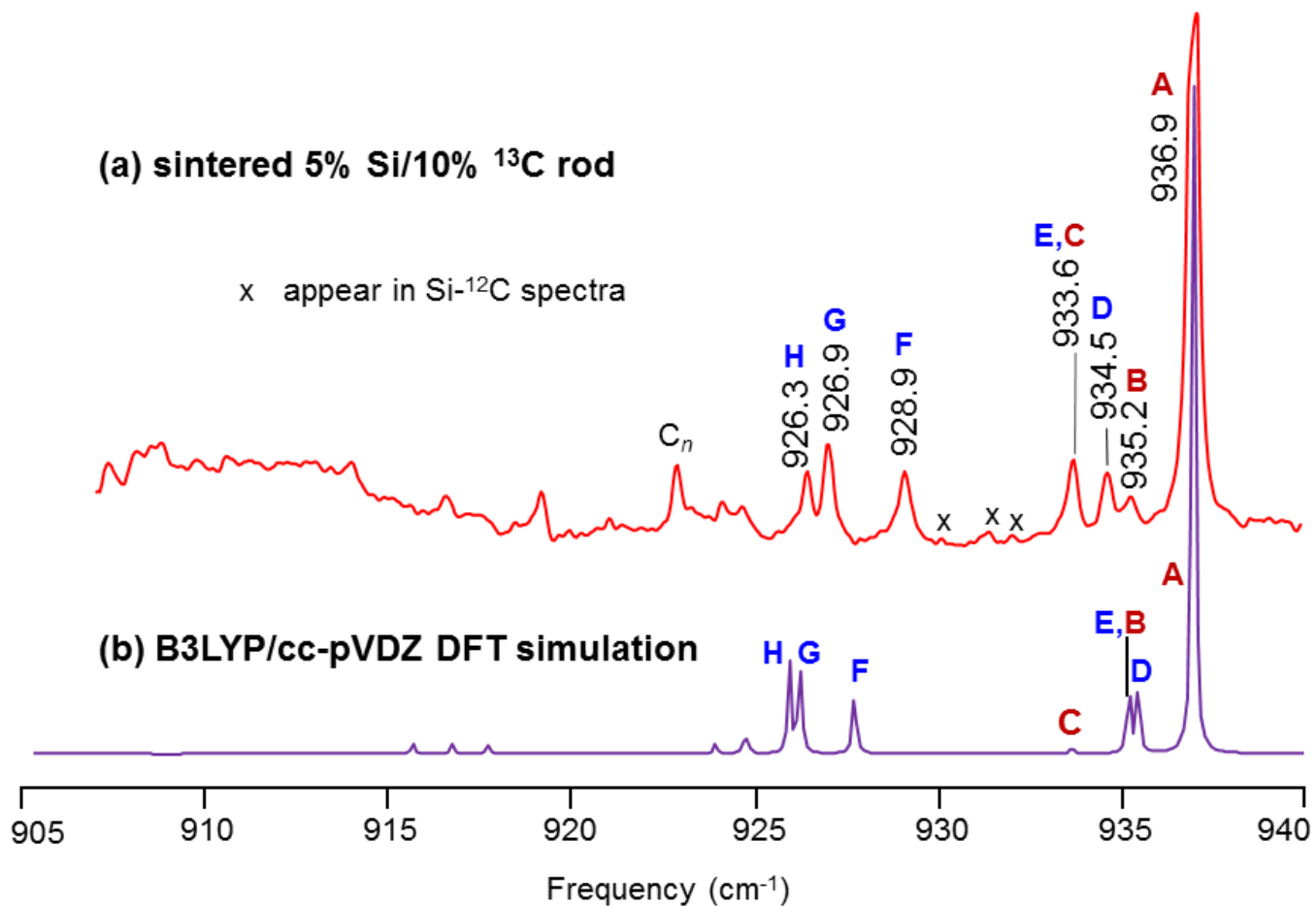


Figure 3.2 Comparison of isotopic shift spectra of the $\nu_4(\sigma)$ mode of linear SiC_5 produced by (a) the ablation of a sintered, mixed 5% Si /10% ^{13}C rod, with a DFT simulation for 10% ^{13}C enrichment, calculated at the (b) B3LYP/cc-pVDZ level. ^{13}C -isotopic shift frequencies and isotopomers in the spectra are labeled according to the list in Table 3.3.

Table 3.3 Comparison of observed ^{29}Si , ^{30}Si and ^{13}C isotopic shift frequencies (cm^{-1}) to DFT-B3LYP/cc-pVDZ predicted isotopic frequencies for the $\nu_4(\sigma)$ mode of linear triplet ($^3\Sigma$) SiC_5 .

Isotopomer		Observed	B3LYP/ cc-pVDZ	Scaled ^a	Difference
Si-C-C-C-C-C		$\nu_{\text{obs}} (\text{cm}^{-1})$	$\nu_{\text{DFT}} (\text{cm}^{-1})$	$\nu_{\text{scaled}} (\text{cm}^{-1})$	$\Delta\nu (\text{cm}^{-1})$
28-12-12-12-12-12	A	936.9	959.9	936.9	...
29 -12-12-12-12-12	B	935.2	958.2	935.2	0.0
30 -12-12-12-12-12	C	933.5	956.6	933.7	0.2
28-12-12-12- 13 -12	D	934.5	958.3	935.4	0.9
28-12-12- 13 -12-12	E	933.6	958.1	935.1	1.5
28-12- 13 -12-12-12	F	928.9	950.3	927.5	-1.4
28- 13 -12-12-12-12	G	926.9	948.8	926.1	-0.8
28-12-12-12-12- 13	H	926.3	948.5	925.8	-0.5

^a The predicted shifts in column 4 have been scaled by a factor of 936.9/977.2.

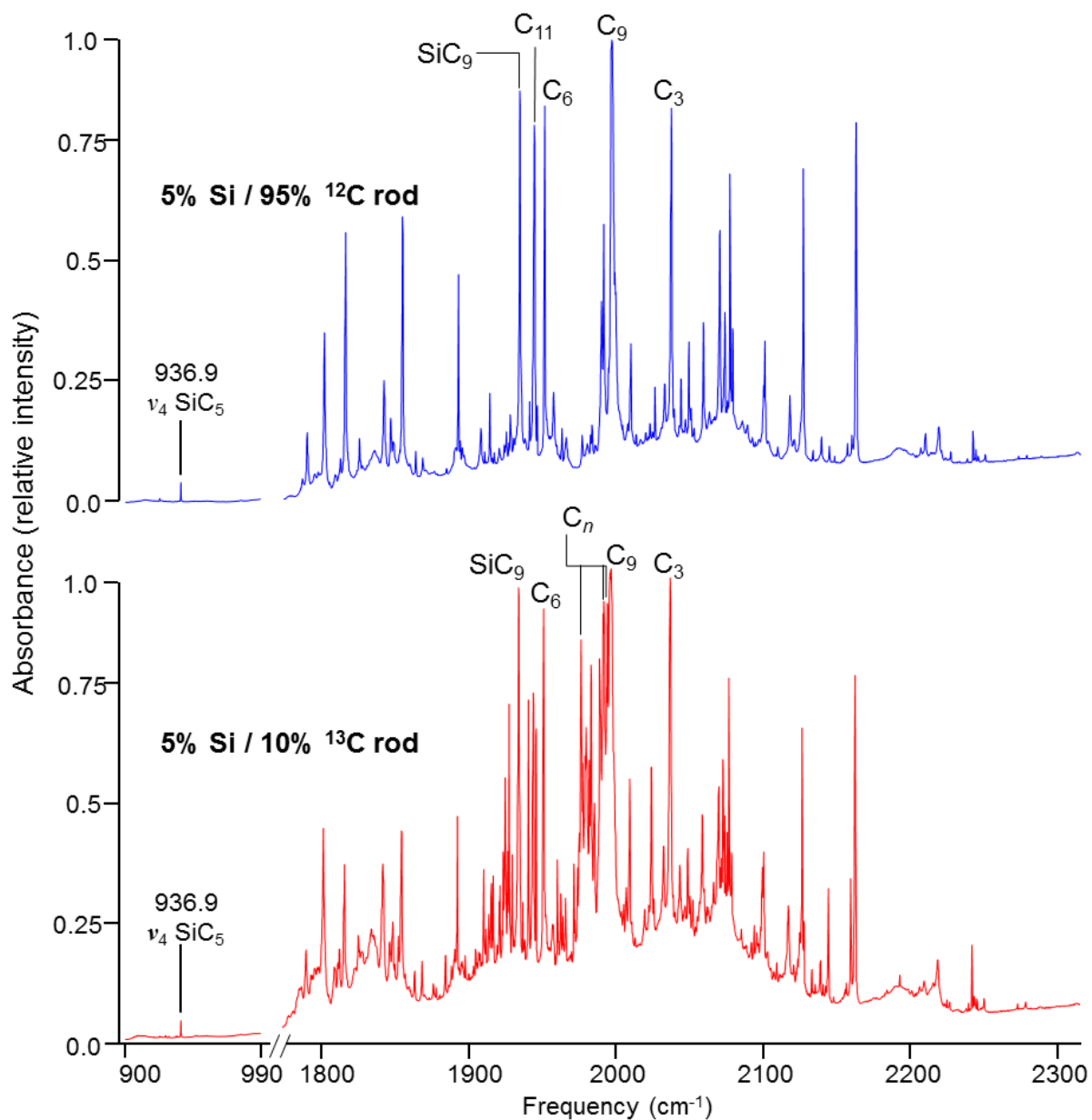


Figure 3.3. FTIR spectra, from 900 to 2300 cm^{-1} , obtained after ablation of a sintered, mixed (a) 5% Si / 95% ^{12}C rod and (b) 5% Si / 10% ^{13}C rod. These spectra are shown to emphasize the difficulty of finding experimental candidates for the ν_1 , and ν_2 modes of SiC_5 .

CHAPTER IV

FTIR IDENTIFICATION OF ν_5 MODE OF SiC_5Si

4.1 INTRODUCTION

Linear, disilicon-carbon Si_2C_n molecules have been the focus of many theoretical and experimental investigations because of their potential applications in the fields of astrophysics, semiconductors, and electronic devices. For example, Kaiser *et al.*⁶² simulated the ablation of micro-meteorites entering Titan's atmosphere by entraining the products from the laser ablation of a Si rod in a supersonic beam of acetylene carrier gas with which they reacted. Si_2C_n ($n = 1-6$) molecules were identified in mass spectra of the products. The role of Si_nC_m molecules has also been considered in the formation of silicon carbide grains that have been found in meteorite samples, and are thought to be produced in the dust driven wind from pulsating carbon-rich asymptotic giant branch stars.⁶³

Si_2C , the simplest disilicon-carbon molecule, was tentatively identified by Weltner and McLeod⁶⁴ by means of 1187 and 1205 cm^{-1} absorptions observed in vibrational infrared spectra of the products from silicon carbide evaporation that were trapped in Ar and Ne matrices. In subsequent FTIR experiments in the TCU Molecular Physics lab trapping the products from the evaporation of a silicon-carbon mixture in solid Ar, Presilla-Márquez *et al.*⁶⁵ confirmed the earlier identification⁶⁶ of the $\nu_3(b_2)$ anti-symmetric, Si-C stretch at 1188.4 cm^{-1} and identified a new fundamental at 839.5 cm^{-1} as the $\nu_1(a_1)$ symmetric Si-Si stretch. The identifications were based on comparison of the ^{13}C isotopic shift spectrum with the predictions of Rittby's second-order many-body perturbation theory (MBPT2) investigation,⁶⁷ which indicated that the ground

state structure has C_{2v} symmetry. Using a similar experimental approach, measuring ^{13}C isotopic shifts and comparing them with the predictions of DFT calculations, the next molecule in the series, Si_2C_2 , was found to have rhombic (1A_g state) geometry and the vibrational fundamentals $\nu_3(b_{1u}) = 982.9$ and $\nu_4(b_{2u}) = 382.2 \text{ cm}^{-1}$ were identified.⁶⁸

With the addition of a third C atom, MBPT(2) calculations predict a linear SiC_3Si geometry is lowest in energy.⁶⁹ The C-C and Si-C fundamentals, respectively, $\nu_3 = 1955.2$ and $\nu_4 = 898.9 \text{ cm}^{-1}$ were identified for this molecule trapped in solid Ar⁷⁰ by comparing ^{13}C and $^{29,30}\text{Si}$ isotopic shift measurements with the predictions of MBPT(2) calculations.⁷¹ Shortly after these identifications, Van Orden *et al.*⁷² reported a gas phase study that used supersonic cluster beam-diode laser spectroscopy to measure to high precision $\nu_3(\sigma_u) = 1968.18831 \text{ cm}^{-1}$. The photoelectron spectrum of the Si_2C_3^- anion produced using a cold cathode discharge was observed by Duan *et al.*⁷³ who assigned the $\nu_1(\sigma_g) = 1520 \pm 25$ and $\nu_2(\sigma_g) = 490 \pm 25 \text{ cm}^{-1}$ modes of linear SiC_3Si in the ground electronic state. More recently, the $(\nu_3 + \nu_7) - \nu_7$ hot band of SiC_3Si has been observed in the gas phase.⁷⁴

The observation of the next molecule in the series SiC_4Si , was reported by this lab in an FTIR study in solid Ar. The linear $^3\Sigma_g^-$ ground state geometry predicted by earlier MBPT(2) calculations using a triple zeta basis with polarization (TZP),⁷⁵ was confirmed. Comparison of all ^{13}C isotopomer frequencies as well as single $^{29,30}\text{Si}$ shifts with the predictions of new DFT calculations using the standard three-parameter Becke 88 exchange functional with Lee-Yang-Parr correlational functional^{76,77,78} (B3LYP) and 6-311G(2d) basis, enabled the identification of the $\nu_4(\sigma_u) = 1807.4$ and $\nu_5(\sigma_u) = 719.1 \text{ cm}^{-1}$ stretching fundamentals.

Up to the present, no further progress in the observation of vibrational spectra of SiC_nSi molecules incorporating longer C_n chains ($n > 4$) has been reported. As already noted, mass

spectrometric evidence of Si_2C_5 has been observed⁶² in the reaction of acetylene with the products from the laser ablation of silicon. DFT-B3LYP/6-311G* calculations by Jiang *et al.*,⁷⁹ predict that the most intense mode of linear SiC_5Si should be $\nu_4(\sigma_u) = 2144 \text{ cm}^{-1}$. Here we report the observation of one and possibly two vibrational fundamentals of linear SiC_5Si .

4.2 EXPERIMENTAL PROCEDURE

SiC_5Si was produced by the laser ablation of a sintered Si/C rod, made from powdered mixtures of Si and C with 30% (by mol) Si content, and pressed at $4.5 \times 10^5 \text{ kPa}$. The Si/C rod was evaporated using a Nd:YAG laser (Spectra Physics) operating at 1064 nm in the pulsed mode. The evaporated species were condensed in solid Ar (Matheson, 99.9995% purity) on a gold surfaced copper mirror enclosed in a vacuum chamber maintained at a pressure of $\sim 10^{-8}$ Torr. The mirror was cooled to $\sim 20 \text{ K}$ by a closed cycle refrigeration system (ARS, Displex). After the products were trapped in solid Ar, FTIR absorption spectra of the samples were recorded using a Bomem DA3.16 Fourier transform spectrometer equipped with KBr beamsplitter and liquid nitrogen cooled Hg-Cd-Te detector, in the range $400 - 3000 \text{ cm}^{-1}$, at a resolution of 0.2 cm^{-1} . Details of the optical system have been reported previously.⁸⁰

In order to analyze the FTIR data and unambiguously identify the molecular structure and vibrational fundamentals of novel molecules, it is essential to study their isotopic shift spectra. Si/C rods were fabricated with a mixture of ^{12}C (Alfa Aesar, 99.9995% purity) and ^{13}C (Isotec, 99.3% purity) in a percent molar ratio of 30% Si / 60% ^{12}C / 10% ^{13}C designed to promote the formation of single ^{13}C -substituted isotopomers. Experimental parameters such as Ar flow, laser power, and laser focus, were varied in order to optimize the production of SiC_5Si . The laser beam with a power of 3.1 W was loosely focused on an area of $\sim 0.5 \text{ cm}^2$ to ablate the sintered Si/C rod. During deposition, the Ar flow rate was adjusted with a needle valve until the chamber

pressure increased from $\sim 10^{-8}$ to 10^{-5} Torr. Typically, matrix samples in the experiments discussed here were deposited in increments of 2 minutes, and up to a total of 30 minutes.

4.3 RESULTS AND ANALYSIS

Potential candidates for Si_nC_m absorptions in the $400 - 3000 \text{ cm}^{-1}$ range were identified by comparing spectra produced by the ablation of a sintered, mixed 30% Si / 70% ^{12}C Si/C rod to spectra produced by pure graphite ablation. Many candidates were found, and in particular, in the $1550 - 1600 \text{ cm}^{-1}$ region, which is relatively clear of crowding bands, a strong, unidentified absorption attributable to a Si_nC_m species was observed at 1590.8 cm^{-1} . Since the spectrum resulting from the Si/C rod ablation exhibits only trace amounts of contaminant species, such as H_2O and CO_2 , it is likely that the absorption belongs to a Si_nC_m molecule. Figure 1(a) shows three weaker bands observed to the low frequency side of the 1590.8 cm^{-1} absorption at 1590.2 , 1589.6 and 1589.1 cm^{-1} . These absorptions could be either modes of other Si_nC_m species, or more likely, Si isotopic shifts from the 1590.8 cm^{-1} absorption. For further analysis, it is necessary to determine the rest of the molecule's composition (e.g. number of C atoms, Si atoms and structure).

For this purpose, experiments using 10% ^{13}C enrichment were carried out to produce predominantly single ^{13}C -substituted isotopomers. Figure 4.2(a) shows three distinct new bands observed to the low frequency side of the 1590.8 cm^{-1} band, at 1588.3 , 1576.5 and 1569.6 cm^{-1} that are candidates for single ^{13}C isotopomer shifts. The relative intensities of the three strong bands are ~ 20 , 10 and 20% of the fundamental, and remain so even after annealing at 27 K for 10 min and at 30 K for 5 min . This behavior is consistent with them all being ^{13}C shifts of the

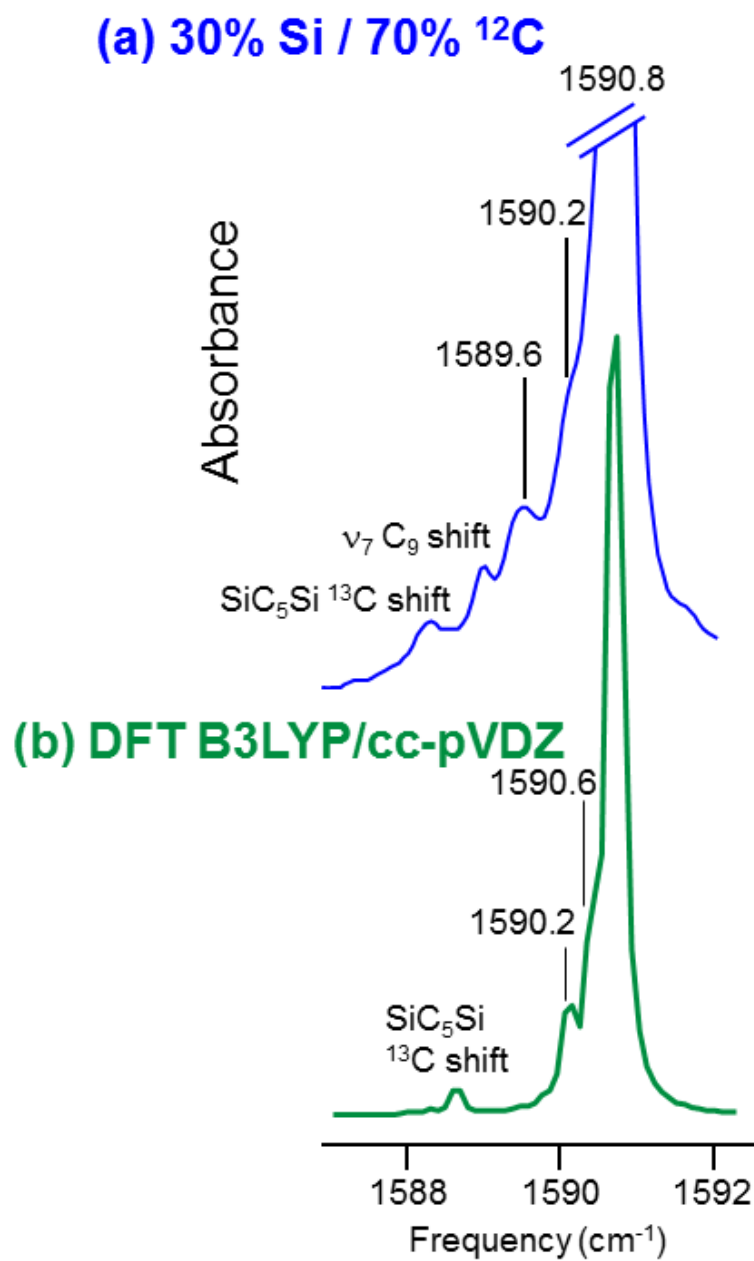


Figure 4.1 Comparison of the FTIR spectra produced by the ablation of (a) graphite rod, (b) a sintered, mixed 30% Si / 70% ^{12}C rod, (c) a DFT simulation at the B3LYP/cc-pVDZ level of the $^{29,30}\text{Si}$ -isotopic shifts for the $\nu_5(\sigma_u)$ mode of linear, triplet SiC_5Si .

1590.8 cm^{-1} fundamental and, consequently, that the carrier contains two pairs of symmetrically equivalent carbon atoms and a central carbon atom. Other weaker absorptions also appear in Figure 4.2(a) that are possible double ^{13}C substituted isotopomers. Increasing the ^{13}C enrichment from 10 to 20% (by mol) resulted in all three bands growing in intensity relative to the 1590.8 cm^{-1} absorption [see . Figure 4.2(b)], confirming that they belong to the same molecule. In addition, the higher enrichment yielded six new absorptions at 1585.9, 1574.9, 1567.9, 1565.8, 1555.8, and 1548.8 cm^{-1} that are candidates for doubly, ^{13}C – substituted isotopomers. Each of these absorptions has a relative intensity of $\sim 10\%$ of the main band's intensity. The band at 1565.8 cm^{-1} may have a contribution from an absorption at the same frequency observed in Figure 4.1(a) in the Si/ ^{12}C experiment. The simplest molecule likely to produce the observed isotopic spectra is linear SiC_5Si , with a chain of five carbon atoms and two terminal Si atoms.

Comparison of the observed ^{13}C isotopic shift spectra with DFT simulated isotopic shift spectra provides the critical test for confirming the identification of SiC_5Si and the assignment of the vibrational fundamental. In the lowest energy ground state, linear SiC_5Si can have singlet or triplet spin multiplicity; however, a DFT calculation using the B3LYP^{76,81,82} functional and (correlation consistent, split valence, double zeta) cc-pVDZ basis⁸³ in the GAUSSIAN 03 suite of programs shows that the energy of the linear triplet form is ~ 28 kcal/mol higher than the linear singlet. Table I gives the calculated frequencies of the vibrational fundamentals for the $^1\Sigma_g^-$ state. Comparison with the observed 1590.8 cm^{-1} frequency suggests that it is a likely candidate for the $\nu_5(\sigma)$ fundamental of SiC_5Si predicted at 1650.0 cm^{-1} .

The ^{13}C isotopic shift spectrum for the 1590.8 cm^{-1} absorption resulting from the ablation of a rod containing a 30% Si / 50% ^{12}C / 20% ^{13}C mixture shown in Figure 4.2 (b). Visual

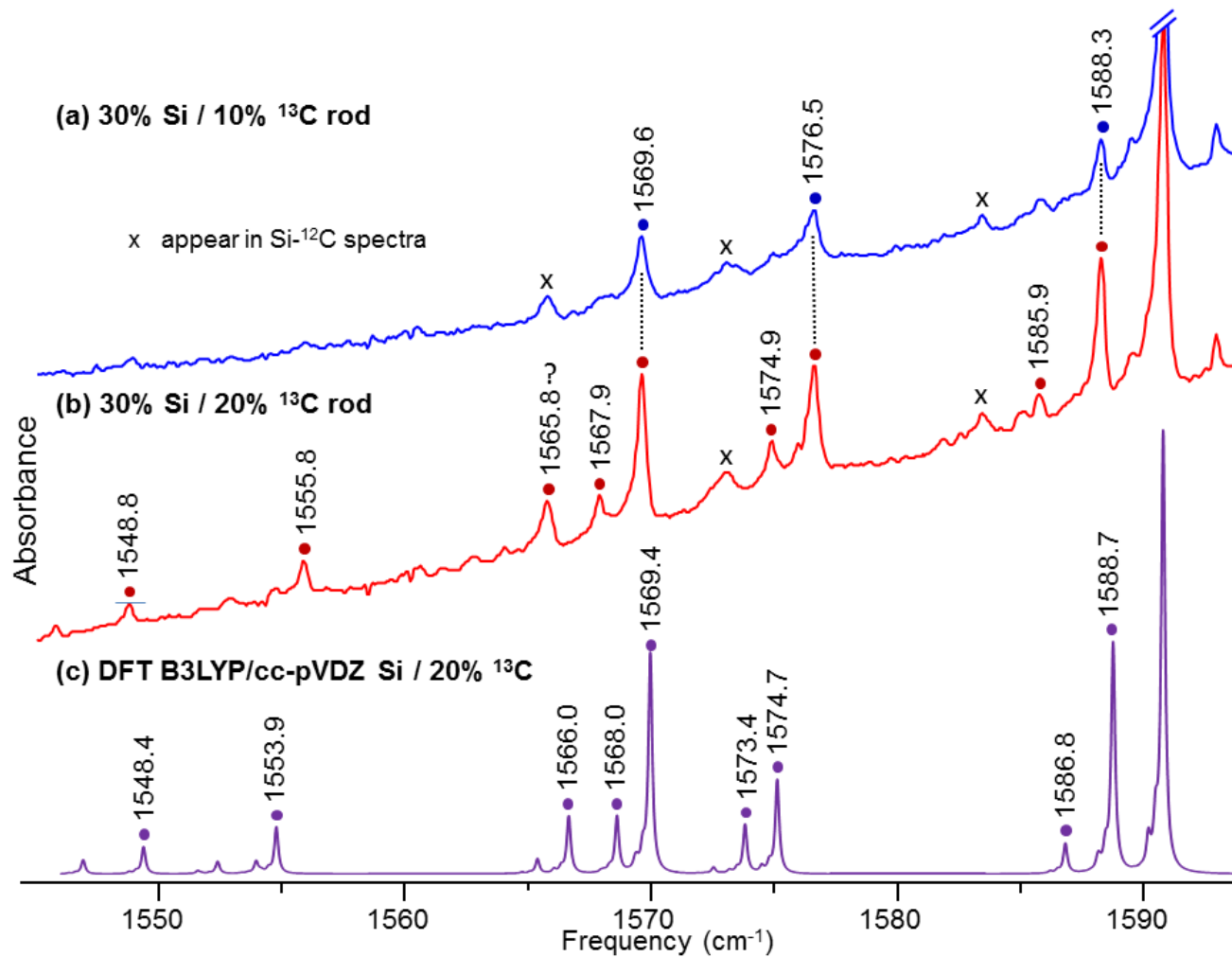


Figure 4.2 Comparison of isotopic shift spectra of the $\nu_5(\sigma_u)$ mode of linear SiC_5 produced by (a) the ablation of a sintered, mixed 30% Si / 10% ^{13}C / 60% ^{12}C rod, (b) the ablation of a sintered, mixed 30% Si / 20% ^{13}C / 50% ^{12}C rod, and with (c) a DFT simulation for 20% ^{13}C enrichment, calculated at the B3LYP/cc-pVDZ level.

Table 4.1. DFT-BVWN5/cc-PVDZ predicted vibrational modes, frequencies (cm^{-1}), and infrared intensities (km/mol) for linear, singlet ($^1\Sigma_g^-$) SiC_5Si .

Vibrational mode	Frequency (cm^{-1})	Infrared intensity (km/mol)
$\nu_1(\sigma_g)$	2042	0
$\nu_2(\sigma_g)$	1156	0
$\nu_3(\sigma_g)$	391	0
$\nu_4(\sigma_u)$	2155	4839
$\nu_5(\sigma_u)$	1650	1265
$\nu_6(\sigma_u)$	720	138
$\nu_7(\pi_g)$	524	0
$\nu_8(\pi_g)$	134	0
$\nu_9(\pi_u)$	627	26
$\nu_{10}(\pi_u)$	247	10
$\nu_{11}(\pi_u)$	52	2

comparison with the DFT-simulated ^{13}C isotopic shift spectrum for the $\nu_5(\sigma_u)$ mode of linear SiC_5Si in Figure 4.2(c) shows very similar isotopic shift patterns. Table II showing a quantitative comparison between observed and calculated frequencies indicates that the discrepancies between the measured and DFT predicted ^{13}C shifts are 1.9 cm^{-1} or less. Similarly, the DFT simulation for the $^{29,30}\text{Si}$ -isotopic shifts shown in Figure 4.1(b) is very close to the observed isotopic shift pattern in Figure 4.2(a). As shown in Table II, the discrepancies between the measured and calculated $^{29,30}\text{Si}$ shift bands are 0.6 and 0.4 cm^{-1} . On the basis of the agreement between the measured and DFT-predicted ^{29}Si , ^{30}Si , and ^{13}C isotopic shifts, the absorption at 1590.8 cm^{-1} can therefore be confidently assigned to the $\nu_5(\sigma_u)$ fundamental of linear SiC_5Si .

As shown in Table I, the DFT-B3LYP/cc-pVDZ calculation predicts the ν_4 vibrational fundamental of linear SiC_5Si at 2155 cm^{-1} with an intensity ~ 4 times more intense than the observed $\nu_5(\sigma_u)$ band. Figure 4.3(a) shows a potential candidate, for the $\nu_4(\sigma_u)$ fundamental, lying at 2021.3 cm^{-1} . Its intensity was measured to be consistently ~ 4 times that of ν_5 . Unfortunately, unambiguous analysis of the isotopic shift pattern for this candidate band is not possible, because it lies in a densely crowded region where the isotopic shift patterns for the C-C stretching fundamentals of C_6 , C_9 , C_3 and other carbon chains overlap.

Figure 4(a) shows the spectrum in the $1965\text{-}2025\text{ cm}^{-1}$ neighborhood of the ν_4 candidate at 2021.3 cm^{-1} that was recorded following the ablation of a 30% Si / 10% ^{13}C rod. For comparison, the DFT-predicted isotopic shift pattern for 20% ^{13}C enrichment is shown in Fig. 4(b). Bands in the observed spectrum belonging to $^{12,13}\text{C}_n$ and Si_nC_m species are marked by green and blue squares, respectively. They were eliminated as potential shifts for $\nu_4(\sigma_u)$ by comparing spectra resulting from the ablation of rods made from $\text{Si}/^{12}\text{C}$, $^{12}\text{C}/^{13}\text{C}$ and $\text{Si}/^{12}\text{C}/^{13}\text{C}$

mixtures with 10 and 20% ^{13}C enrichment levels. Of the remaining bands those denoted with red dots grew in intensity with the higher 20% ^{13}C enrichment, and are thus potential shift bands for the ν_4 candidate at 2021.3 cm^{-1} . Specifically, the band observed at 2020.3 cm^{-1} and pairs of bands at ~ 2008 and $\sim 1983\text{ cm}^{-1}$ [Fig. 4(a)] are close to the shift bands at 2019.9 , 2006.4 , and 1984.8 cm^{-1} [Fig. 4(b)] predicted for single ^{13}C substitutions at the 2 equivalent and unique central C sites in SiC_5Si . Unfortunately, extensive annealing experiments to test for multiple trapping sites did not simplify the spectrum. Although there is no basis for selecting a specific member of either pair, a comparison in Table III between the frequencies predicted for the single ^{13}C shifts and the 2 pairs of observed frequencies, shows that the largest discrepancy is 2.3 cm^{-1} . Weaker bands appearing to the low frequency side of the three single ^{13}C shift bands and the 1971.0 cm^{-1} band in the DFT simulated spectrum are the shifts for double and triple substitutions, respectively; however, it is not possible to identify them with certainty in the measured spectrum. Moreover, it is very likely that the experimental spectrum includes overlapping bands from other unidentified Si_nC_m species, in particular, those responsible for strong bands at 1991.2 and 1992.9 cm^{-1} shown in Fig. 4(a) and a third absorption at 2045.0 cm^{-1} , in Fig. 3(b). Thus, the identification of the observed 2021.3 cm^{-1} absorption as the $\nu_4(\sigma_u)$ fundamental of SiC_5Si must be regarded as very tentative.

4.4 CONCLUSION

A new absorption at 1590.8 cm^{-1} has been observed in FTIR spectra of the products from the laser evaporation of a silicon/carbon rod trapped in solid Ar. Analysis of the shift spectrum for single ^{13}C substitutions observed with 10% isotopic enrichment indicates that the carrier molecule has 2 pairs of equivalent carbon atoms and one central carbon atom, for which the simplest structure is linear SiC_5Si . DFT-B3LYP/cc-pVDZ calculations predict that the ν_4 and ν_5 modes of linear ($^1\Sigma_g^-$) SiC_5Si should be the most intense. Comparison of measured ^{13}C and

^{29,30}Si shifts with DFT predicted frequencies enables the definite identification of the $\nu_5(\sigma_u)$ fundamental at 1590.8 cm^{-1} , but ¹³C shift measurements in a crowded spectral region provide only a tentative assignment for $\nu_4(\sigma_u)$ at 2021.3 cm^{-1} .

Table 4.2. Comparison of observed ^{29}Si , ^{30}Si and ^{13}C isotopic shift frequencies (cm^{-1}) to DFT-B3LYP/cc-pVDZ predicted isotopic frequencies for the $\nu_5(\sigma_u)$ mode of linear, singlet ($^1\Sigma_g^-$) SiC_5Si .

Isotopomer	Observed	B3LYP/ cc-pVDZ	Scaled ^a	Difference
Si-C-C-C-C-C-Si	$\nu_{\text{obs}} (\text{cm}^{-1})$	$\nu_{\text{DFT}} (\text{cm}^{-1})$	$\nu_{\text{scaled}} (\text{cm}^{-1})$	$\Delta\nu (\text{cm}^{-1})$
28-...-28	1590.8	1650.0	1590.8	...
28-...- 29	1590.2	1649.7	1590.6	0.4
28-...- 30	1589.6	1649.4	1590.2	0.6
12- 13 -12-12-12	1588.3	1647.8	1588.7	0.4
12-12- 13 -12-12	1576.5	1633.3	1574.7	-1.8
13 -12-12-12-12	1569.6	1627.8	1569.4	-0.2
12- 13 -12- 13 -12	1585.9	1645.8	1586.8	0.9
12- 13 - 13 -12-12	1574.9	1632.0	1573.4	-1.5
13 -12-12- 13 -12	1567.9	1626.4	1568.0	0.1
13 - 13 -12-12-12	1565.8?	1624.3	1566.0	0.2
13 -12- 13 -12-12	1555.8	1611.7	1553.9	-1.9
13 -12-12-12- 13	1548.8	1606.0	1548.4	-0.4

^a The predicted shifts in column 4 have been scaled by a factor of 1590.8/1650.0 .

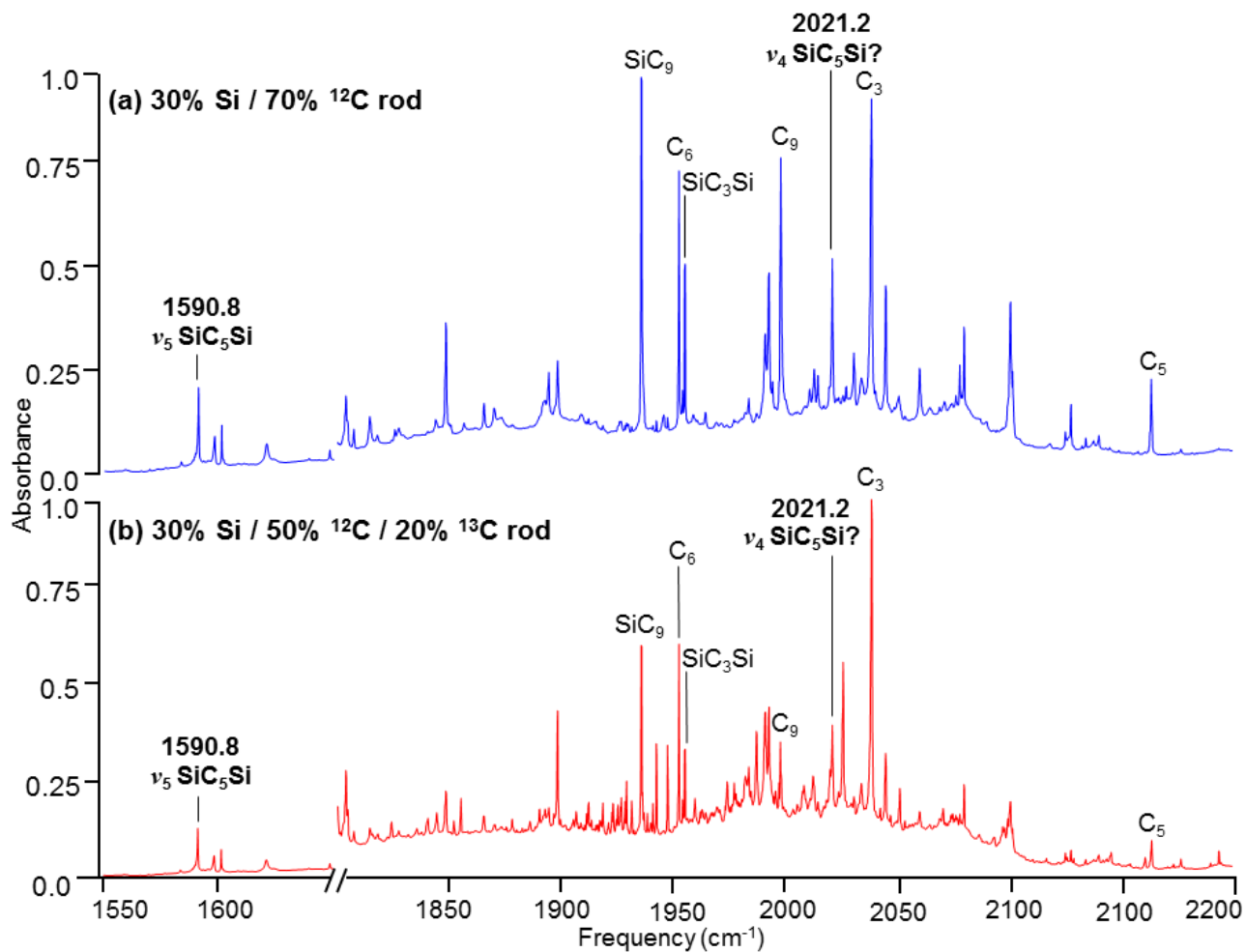


Figure 4.3 FTIR spectra, from 1550 to 2200 cm⁻¹, obtained after (a) ablation of sintered, mixed 30% Si / 70% ¹²C rod and (b) ablation of sintered, mixed 30% Si / 20% ¹³C rod. These spectra are shown to emphasize the difficulty of analyzing the isotopic shift pattern of the observed candidate, 2021.0 cm⁻¹ for the ν_4 mode of SiC₅Si.

Table 4.3. Comparison of observed ^{13}C isotopomer frequencies (cm^{-1}) to DFT-B3LYP/cc-pVDZ predicted singly-substituted isotopic frequencies for the $\nu_4(\sigma_u)$ mode of linear, singlet ($^1\Sigma_g^-$) SiC_5Si .

Isotopomer	Observed ^a	B3LYP/ cc-pVDZ	Scaled ^b	Difference
Si-C-C-C-C-C-Si	$\nu_{\text{obs}} (\text{cm}^{-1})$	$\nu_{\text{DFT}} (\text{cm}^{-1})$	$\nu_{\text{scaled}} (\text{cm}^{-1})$	$\Delta\nu (\text{cm}^{-1})$
12-12-12-12-12	2021.3	2154.9	2021.3	...
13 -12-12-12-12	2020.3	2153.4	2019.9	-0.4
12- 13 -12-12-12	2008.6 2007.8	2139.0	2006.4	-2.2 -1.4
12-12- 13 -12-12	1983.8 1982.5	2116.0	1984.8	1.0 2.3

^a More than one frequency listed indicates that the isotopomer has multiple observed candidates.

^b The predicted shifts in column 4 have been scaled by a factor of 2021.0/2154.9 .

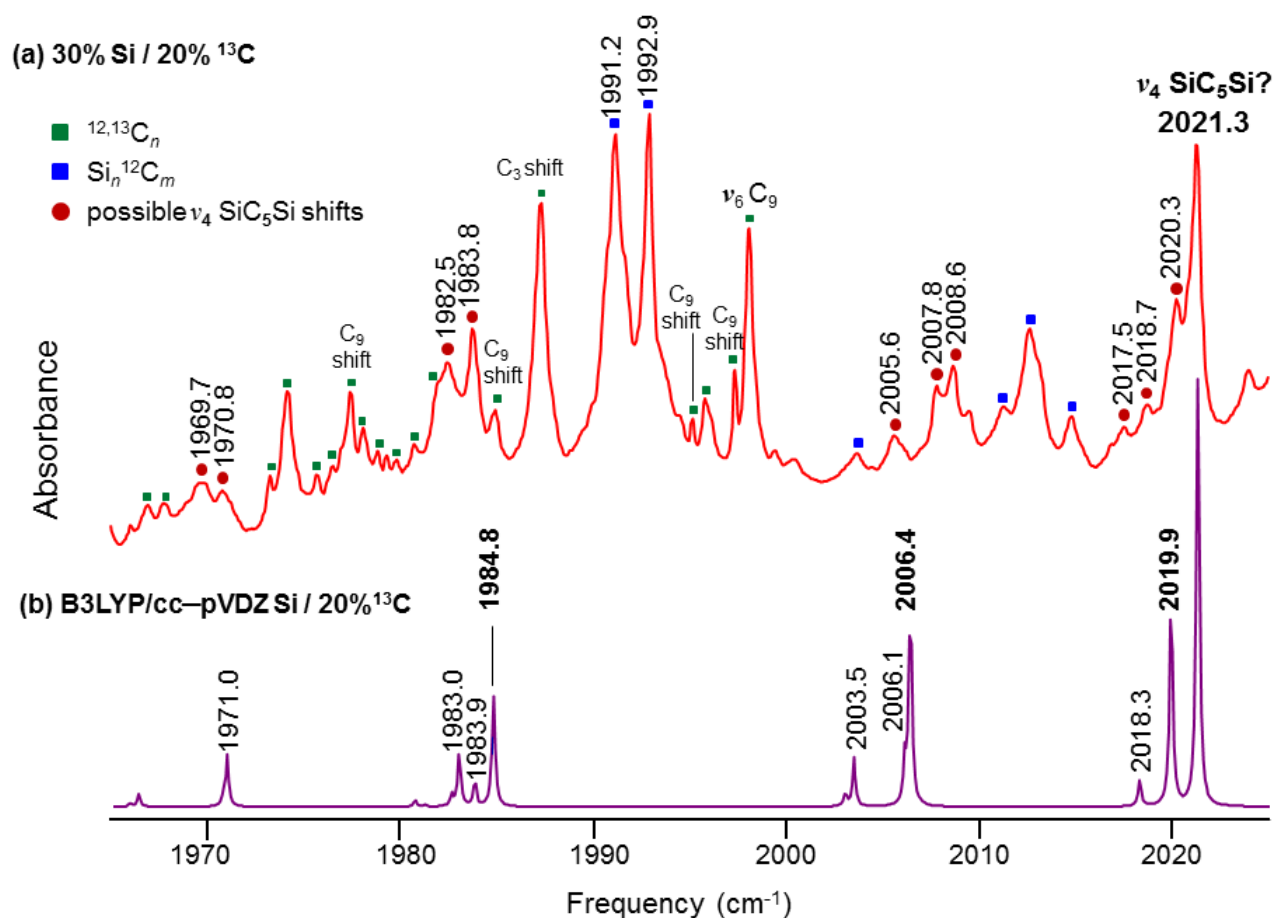


Figure 4.4 FTIR spectra, from 1965 to 2025 cm^{-1} , obtained after (a) ablation of sintered, mixed 30% Si / 20% ^{13}C experiment and (b) a DFT simulation for Si / 20% ^{13}C enrichment, calculated at the B3LYP/cc-pVDZ level, which has been scaled by 2021.3/2155.0. Absorptions that are identified to be $^{12,13}\text{C}_n$ are marked by green squares. Absorptions that are identified to be Si_nC_m are marked by blue squares. Candidates for ν_4 isotopomers of SiC_5Si are marked by red circles.

CHAPTER V

UNIDENTIFIED ABSORPTIONS

5.1 1848.2 cm⁻¹

An unidentified band at 1848.2 cm⁻¹ was observed in the laser ablation of a soft carbon rod, made from powdered mixtures with 30% (by mol) Si content, and pressed at 4.5×10^5 kPa. As an aside, the nearby 1817.8 cm⁻¹ absorption that appears in the graphite only spectrum, is probably an as-yet-unidentified C_n band^a. The laser beam with a power of 2.5 W was loosely focused on an area of ~0.8 cm². Matrix samples in these experiments were deposited in 10 minute increments for a total of 30 minutes. By comparing spectra produced by the ablation of a soft, mixed Si/C rod to spectra produced by pure graphite ablation, the 1848.2 cm⁻¹ band can be considered a potential candidate for a Si-bearing absorption (Figure 5.1). However, further analysis requires a study of the isotopic shift pattern that belongs to this unidentified species.

Figure 5.1(c) shows the spectrum from an experiment with Si/C rod fabricated with a mixture of 30% Si / 60% ¹²C / 10% ¹³C. On enriching the rod with ¹³C, three bands shifted from 1848.2 cm⁻¹ are observed at 1844.3, 1840.2 and 1824.0 cm⁻¹. Then increasing this enrichment from 10% to 20% ¹³C (by mol), all three bands increased their intensity with respect to the 1848.2 cm⁻¹ absorption, implying that they are shifts of the same molecular species [see Figure 5.1(d)]. In the spectrum of the 10% ¹³C enriched sample, the intensity of each presumed

^a In subsequent ¹³C experiments, isotopic shifts for this unidentified C_n band were not observed.

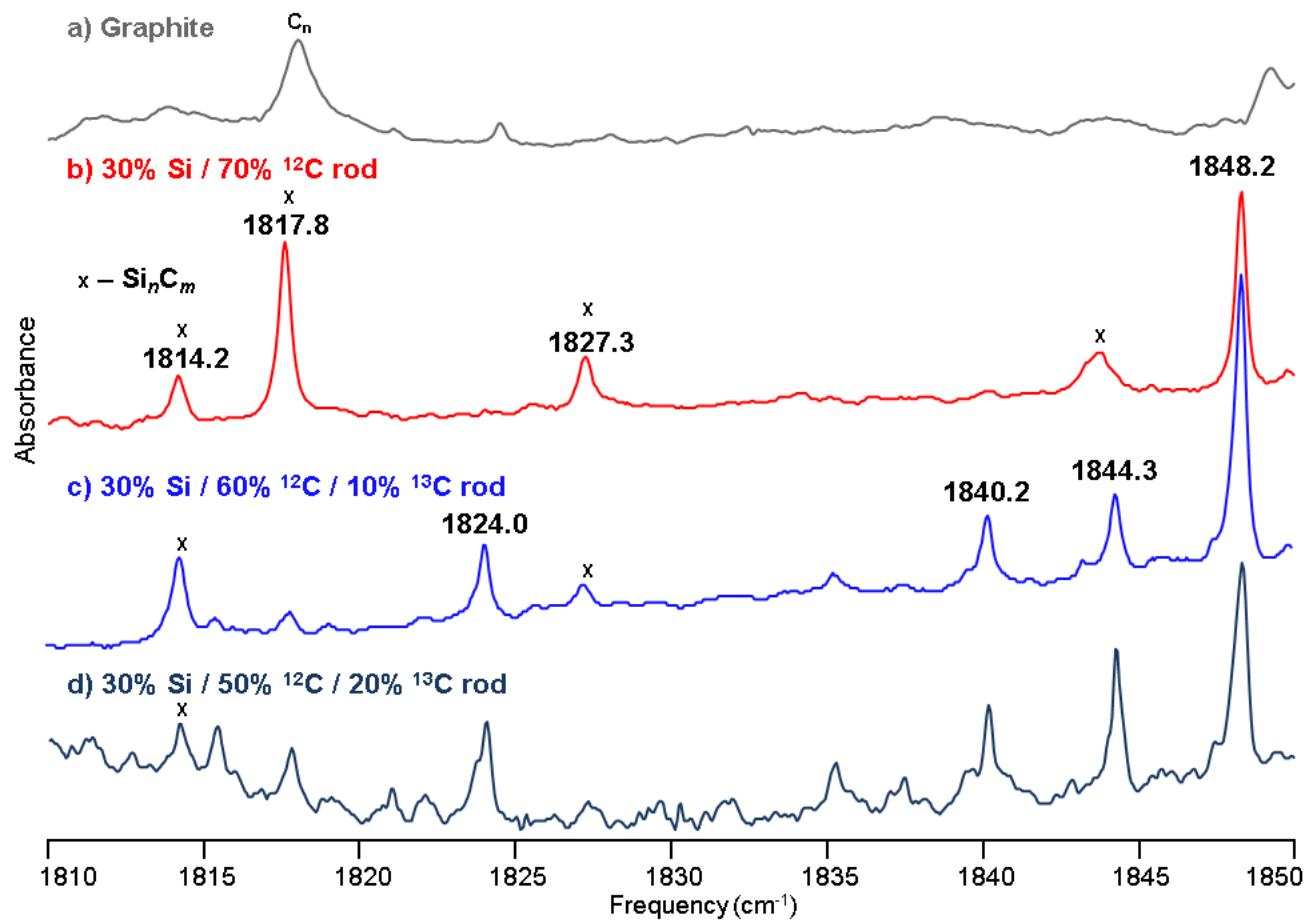


Figure 5.1 Comparison of FTIR spectra produced by the ablation of (a) a graphite rod, (b) a soft 30% Si / 70% ^{12}C (by mol) rod, (c) a soft 30% Si / 60% ^{12}C / 10% ^{13}C rod, and (d) a soft 30% Si / 50% ^{12}C / 20% ^{13}C rod. The bands marked by the symbol “x” are Si_nC_m absorptions.

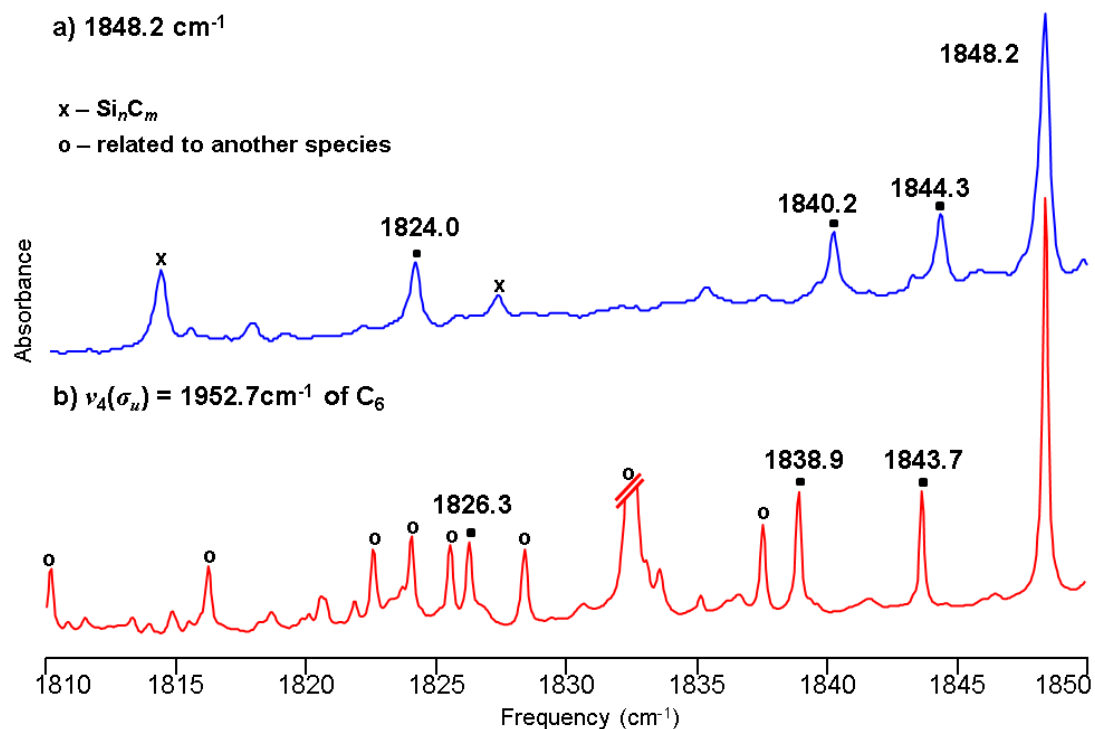


Figure 5.2 Comparison of the ¹³C shift spectra observed for (a) the 1848.2 cm⁻¹ absorption and for (b) the ν₄(σ_u) = 1957.2 cm⁻¹ band of C₆, produced in both cases by the ablation of a soft, 30% Si / 60% ¹²C / 10% ¹³C rod. The spectrum in (b) has been scaled by 1848.2 / 1952.7 cm⁻¹. Absorptions that are identified to be Si_nC_m are marked by “x.” Absorptions that are identified to belong to a species other than C₆ in (b) are marked by “o.” Singly-substituted isotopic shift bands of 1848.2 cm⁻¹ and C₆ are marked by squares. The differences between corresponding singly-substituted, isotopic shift bands are 2.3, 1.3 and 0.6 cm⁻¹ (from low to high frequency bands).

isotopomer band is ~20% relative to the fundamental 1848.2 cm^{-1} . This is twice what we would expect for isotopomers with single ^{13}C substitution at inequivalent sites, and indicates that each band corresponds to a pair of equivalent carbon atoms. Therefore, the unidentified molecule likely has 3 pairs of equivalent carbon atoms and we can conclude that the carrier bears a C_6 chain.

Molecules associated with a C_6 chain will likely have isotopic shift patterns similar to that of C_6 . Referring to previous extensive research^{84,85} on the vibrational spectrum of C_6 , we can compare the ^{13}C isotopic shift spectrum for 1848.2 cm^{-1} to that of the $\nu_4(\sigma_u) = 1952.7\text{ cm}^{-1}$ of C_6 (its most intense vibrational mode) in Figure 5.2. The differences between corresponding isotopomer bands (from low frequency to high frequency bands) are 2.3, 1.3 and 0.6 cm^{-1} . These differences are small and further support the assignment of 1848.2 cm^{-1} to a molecule with a C_6 chain. In addition, 1848.2 cm^{-1} cannot be a new vibrational mode of C_6 . DFT-B3LYP/cc-pVDZ calculations for C_6 show that there are only two IR active vibrational modes in the ~ 1000 - 2000 cm^{-1} region. These are ν_4 and ν_5 , which were identified at 1197.3 and 1952.5 cm^{-1} by Kranze *et al.* in this lab.⁸⁴

A comparison between the observed spectra of 1848.2 cm^{-1} with DFT predictions is necessary to precisely identify the molecular structure of the carrier of 1848.2 cm^{-1} . Because 1848.2 cm^{-1} was observed in the ablation of Si/C rod and not in carbon only experiments, calculations were carried out for the potential candidate SiC_6Si . In the ground state, SiC_6Si is most likely to have a spin multiplicity of one or three, and our DFT-B3LYP/cc-pVDZ calculations showed that the singlet linear form has energy that is $\sim 9\text{ kcal/mol}$ greater than the triplet linear. This is a small difference. However, a theoretical study reported by Jiang *et al.* using DFT-B3LYP/6-311g* also found the triplet state to be lower in energy than the singlet state³⁵. Moreover, they found that for SiC_nSi ($n = 2-11$), when n is odd, the more stable state has multiplicity of 1 and when n

is even, the more stable state has a multiplicity of 3. The consequent calculations for the vibrational modes for the triplet linear form are shown in Table 1.1. From this table, the most intense mode is predicted to be at 2079 cm^{-1} , which is 231 cm^{-1} different from 1848.2 cm^{-1} and is a very large difference. (Similarly, for the singlet state, the most intense mode is predicted at 2078 cm^{-1} .) In addition, previously identified stretching modes of long chain C_n and Si_2C_n species have had discrepancies that range from 1 to 7% (see Table 5.2), so experimental observations are usually very close to theoretical calculations. In contrast, the 231 cm^{-1} difference between the SiC_6Si DFT calculation and 1848.1 cm^{-1} is a 12.5% discrepancy. This unusually large difference and the presence of a contaminant band at 2234.0 cm^{-1} that belongs to C_3O warrants reconsideration of what species could be the carrier of the 1848.2 cm^{-1} band.

Four considerations were made regarding other possible species that could be the carrier of 1848.2 cm^{-1} . In the first consideration, experiments were redone in attempt to produce as clean a sample as is possible; by “clean”, we mean free of any contaminated species (*i.e.* H_2O , C_3O , SiH_2 , C_2O , etc.). Actions were taken such as having the Ar delivery system cleaned out before and after each experiment, sintering mixed powdered rods at $\sim 1663\text{ K}$ ($1390\text{ }^\circ\text{C}$) for several days, and pumping the ablation chamber down to 10^{-8} torr, 30 minutes after which, the gold-plated mirror is cooled down to 20 K . Unfortunately, in these experiments the C_3O band remained a strong absorption. Moreover, a review of past data recorded by other experimentalists in this lab shows that the band C_3O appeared in almost all experiments. In the few past experiments where C_3O did not appear, other contaminants were present with strong intensity.

The second consideration is that the 1848.2 cm^{-1} could possibly belong to different Si_nC_m molecule (*e.g.* SiC_7Si , SiC_8Si , etc.). However, DFT calculations did not result in a fundamental

Table 5.1. DFT-B3LYP/cc-pVDZ predicted vibrational modes, frequencies (cm^{-1}), and infrared intensities (km/mol) for linear, triplet (${}^3\Sigma_g^-$) SiC_6Si .

Vibrational Mode	Frequency (cm^{-1})	Infrared intensity (km/mol)
$\omega_1(\sigma_g)$	2067	0
$\omega_2(\sigma_g)$	1837	0
$\omega_3(\sigma_g)$	980	0
$\omega_4(\sigma_g)$	355	0
$\omega_5(\sigma_u)$	2078	515
$\omega_6(\sigma_u)$	1421	133
$\omega_7(\sigma_u)$	623	23
$\omega_8(\pi_g)$	620	0
$\omega_9(\pi_u)$	534	8
$\omega_{10}(\pi_g)$	355	0
$\omega_{11}(\pi_u)$	219	6
$\omega_{12}(\pi_g)$	117	0
$\omega_{13}(\pi_u)$	44	0

Table 5.2 Comparison of DFT- B3LYP/cc-pVDZ calculations and observed vibrational modes for previously reported centrosymmetric molecules.

Molecule	Vibrational Mode	B3LYP/ cc-pVDZ (cm ⁻¹)	Observed (cm ⁻¹)	Difference (cm ⁻¹)	% difference
SiC ₆ Si	5	2079	1848.2?	231	12.5
SiC ₄ Si	4	1859	1807.4	52	2.9
SiC ₃ Si	3	2052	1955.2	97	5.0
GeC ₃ Ge	3	2028	1920.7	107	5.6
GeC ₅ Ge	4	2135	2158	-23	-1.1
C ₃	3	2157	2038.9	118	5.8
C ₅	3	2270	2164.3	106	4.9
C ₆	4	2038	1952	86	4.4
C ₇	4	2250	2127.8	130	6.1
C ₉	6	2132	1998	134	6.7
C ₁₁	7	2126	1946.0 ± 0.8	180	9.0
C ₁₂	8	2113	1997.3	116	5.8

that had an isotopic shift pattern (see Figure 1.1) that is similar to the isotopic shift pattern of 1848.2 cm^{-1} . Third, it could be that the DFT calculations for SiC_6Si have an unusually larger amount of uncertainty than previous calculations for similar species. The comparison in Figure 5.4 shows the DFT calculations for the vibrational modes of SiC_nSi , n is even. There are two general patterns in this graph. One pattern is that as n increases from 2 to 14, the lowest frequency modes decrease in value (i.e. from 473 to 221 cm^{-1}). Similar behavior occurs for higher frequency modes. The second pattern is that the high frequency modes above $\sim 2000\text{ cm}^{-1}$ form nearly degenerate frequencies, and appear to approach an asymptote near 2200 cm^{-1} . These two patterns also appear for when n is odd (Figure 5.5). In trying to identify the 1848.2 cm^{-1} , we need to know if for $n = 6$, DFT-B3LYP/cc-pVDZ calculations show any unusual behavior. Figure 5.4 shows that when $n = 6$, the frequency modes conform to both the two patterns previously discussed. In addition, Figure 5.6 shows calculated C-C bond lengths for SiC_nSi . Here, the C-C bonds length form an alternating pattern, and for the case $n = 6$, the molecule conforms to this pattern. This eliminates the possibility that the DFT calculation has an unusually, larger amount of uncertainty.

Last, if a pure Si_nC_m is not a good candidate for 1848.2 cm^{-1} , then perhaps a “contaminated” species may be responsible. By “contaminated” we mean silicon or carbon bearing molecules that contain hydrogen, oxygen or nitrogen. Thus calculations for species, such as HSiC_6Si , NC_6N , and $\text{O}_2\text{Si}_2\text{C}_6$, were done to look for vibrational modes that have an isotopic shift pattern like that of the 1848.2 cm^{-1} . The species for which no match was found are not shown here. Table 5.3 lists four “contaminant-bearing” candidate species that were found to have a fundamental for which DFT predicts an isotopic shift pattern similar to that of the band 1848.2 cm^{-1} . Table 5.4, numerically, and Figure 5.7, visually, compare the simulated isotopic

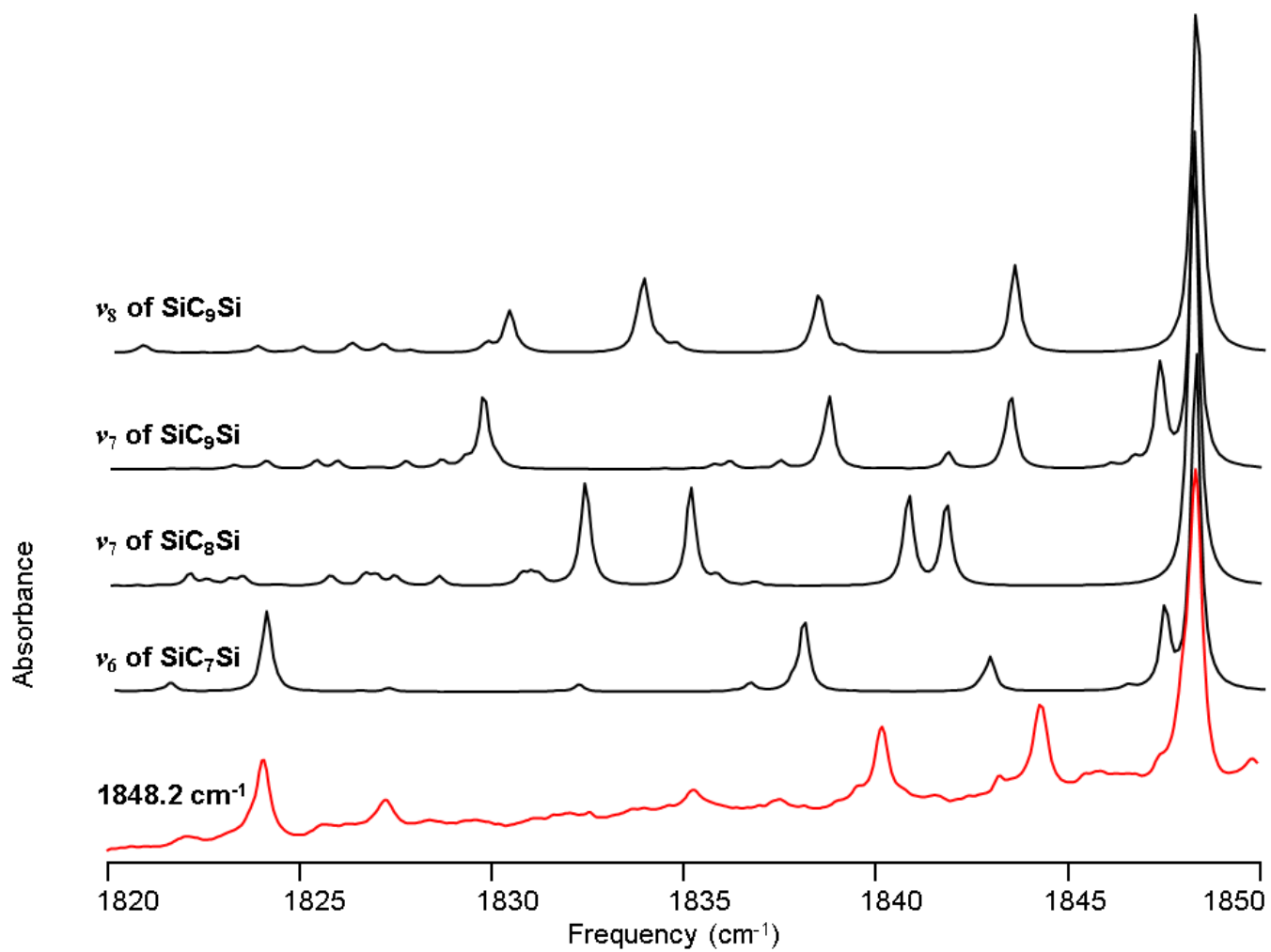


Figure 5.3. Comparison of DFT simulated isotopic shift patterns for ν_8 and ν_7 of SiC_9Si , ν_7 of SiC_8Si , ν_6 of SiC_7Si with the observed isotopic shift pattern of 1848.2 cm^{-1} . This comparison shows that none of these SiC_nSi species could be the carrier for 1848.2 cm^{-1} .

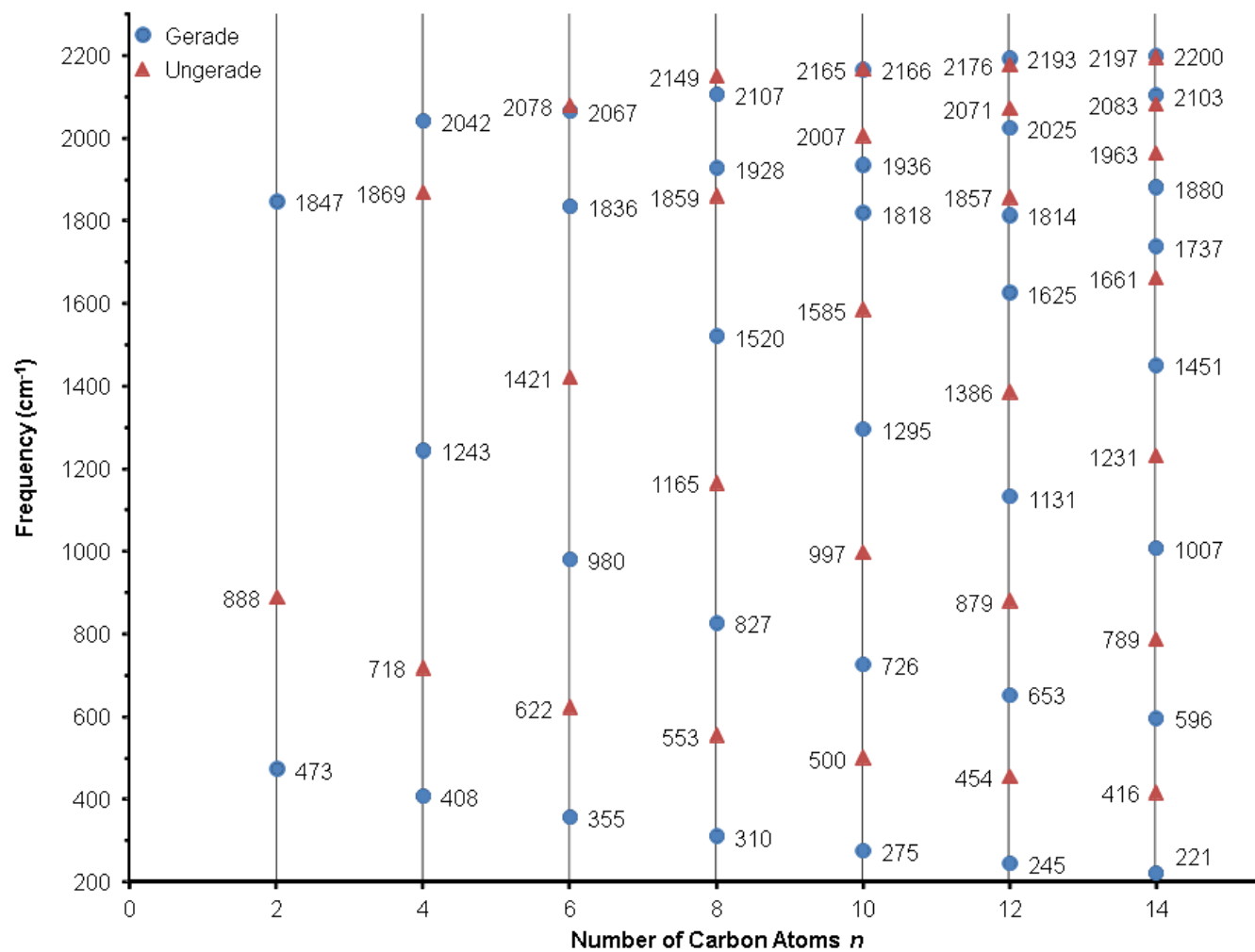


Figure 5.4. Comparison of the DFT-B3LYP/cc-pVDZ calculations for the vibrational stretching modes of SiC_{*n*}Si, where *n* is even.

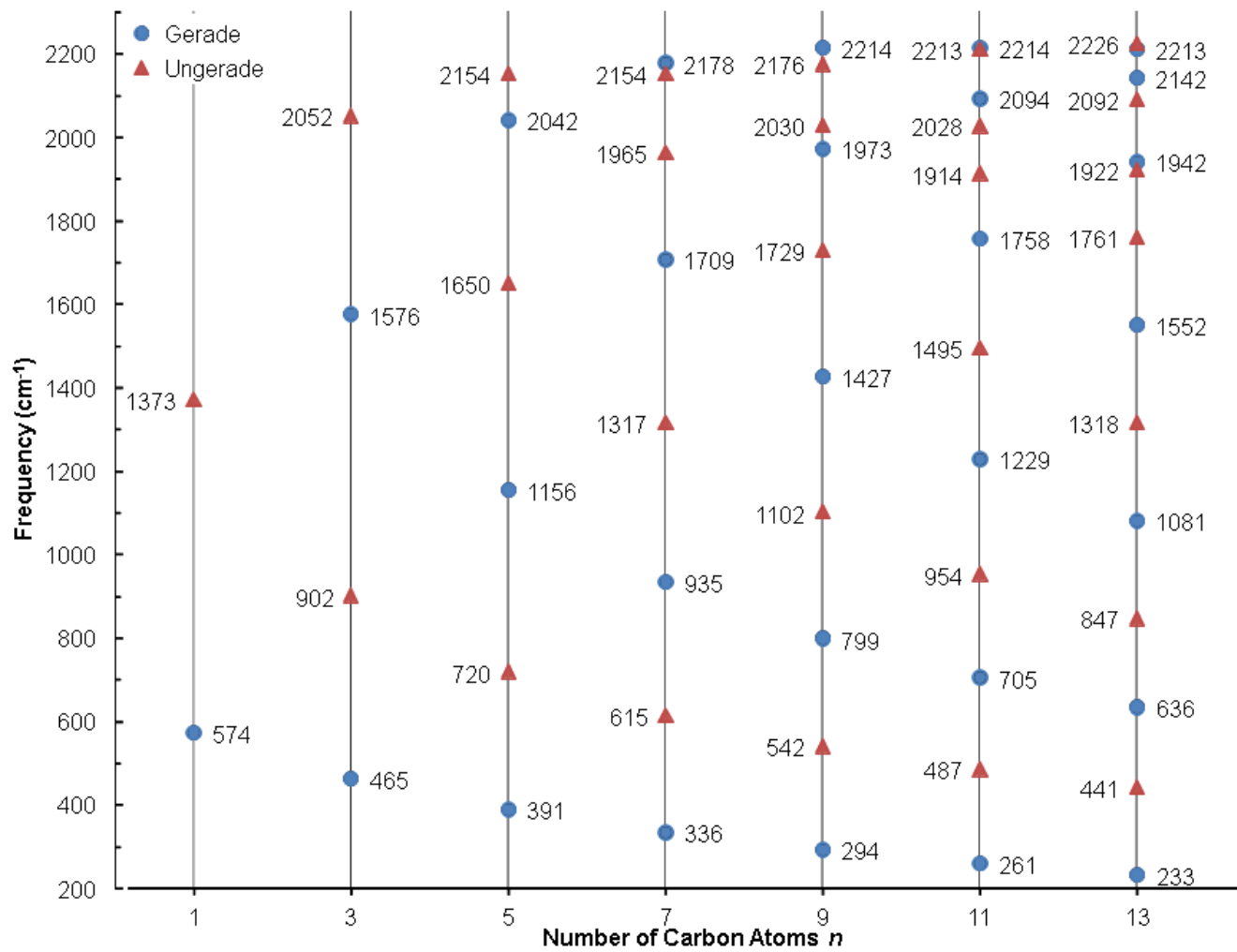


Figure 5.5. Comparison of the DFT-B3LYP/cc-pVDZ calculations for the vibrational stretching modes of SiC_nSi, where *n* is odd.

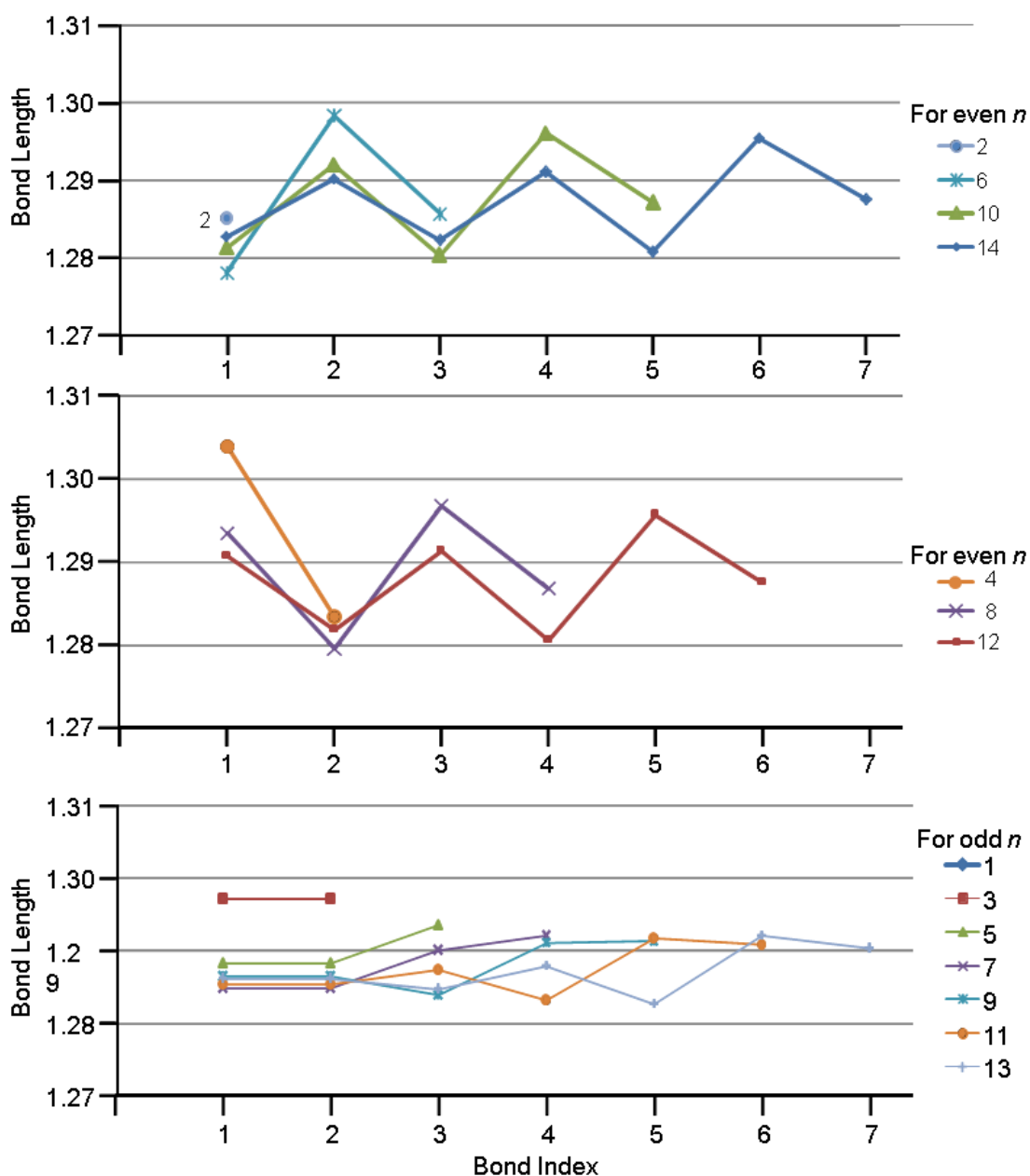


Figure 5.6 Bond lengths (Å) for SiC_nSi calculated using DFT-B3LYP/cc-pVDZ. The bond indices indicate the location of the bond within the molecule. For even n , index 1 is the central bond and the largest index is the terminal bond. For odd n , index 1 and 2 are bonds connected to the central atom. In comparison to the other bond length calculations, when $n = 6$, the bond lengths behave similarly by alternating between shorter and longer lengths. There doesn't appear to be any unusual behavior when $n = 6$.

Table 5.3 Candidate species for the 1848.2 cm⁻¹ band. They are listed with the corresponding DFT-B3LYP/cc-pVDZ predicted vibrational mode, frequency, and multiplicity. These candidate species were calculated to have an isotopic shift pattern similar to that of 1848.2 cm⁻¹.

Molecule	Multiplicity	Vibrational Mode	Frequency (cm ⁻¹)	Difference from 1848.2 (cm ⁻¹)
SiC ₆ Si	3	5	2078	230
NC ₆ N	3	6	1800	48
OSiC ₆ SiO	1	14	2084	236
SiOC ₆ OSi	1	17	2109	261

Table 5.4 Differences between the calculated isotopomer shift bands for different candidate species and the corresponding observed isotopomer bands belonging to 1848.2 cm⁻¹. These candidate species were calculated to have an isotopic shift pattern similar to that of 1848.2 cm⁻¹. The numerical similarities between these simulations and the observed isotopic shift pattern, leaves the question of what carrier is responsible for the 1848.2 cm⁻¹ absorption open.

Molecule	Difference from observed isotopomer band (cm ⁻¹)		
	1844.3	1840.2	1824.0
SiC ₆ Si	-1.6	1.0	1.1
NC ₆ N	0.3	-2.3	0.7
OSiC ₆ SiO	-0.4	0.4	1.1
SiOC ₆ OSi	-0.1	-0.2	0.9

shift patterns with that of 1848.2 cm^{-1} . (As an aside, in Figure 5.7(a) there is a near-lying absorption in the simulation for OSiC_6SiO at 1839.1 cm^{-1} .) These calculated isotopomer bands all have discrepancies that are less than 2 cm^{-1} from the observed isotopic shifts, and therefore, does not help narrow down the list of possible carriers. In addition, DFT calculations for predicts the presence of stronger intensity fundamentals lying in other regions of the spectrum. If candidates for some of these bands were observed, it would help to narrow down the list of possible carriers. For C_6N_2 , there was calculated a band, of similar intensity to 1800 cm^{-1} , at 1940 cm^{-1} . For SiOC_6OSi , there was calculated a bending mode at 893 cm^{-1} , with intensity almost 250 times that of the candidate 2109 cm^{-1} . Similarly, for OSiCSiO , the species was calculated to have three stronger modes at 185 , 483 and 1164 cm^{-1} and with intensity estimates that were all more than 80 times the intensity approximation of the candidate 2084 cm^{-1} . Experimentally observed absorptions were not found for all of these stronger intensity modes. Also, in part because some of the lower frequency modes lie outside of the spectral range of the MCT detector. However, not being able to find candidates for these stronger bands is does not necessarily mean the species can't be present, because DFT intensity calculations have a large amount of uncertainty. (A previous study on a long chain molecule C_{12} discusses the uncertainty of intensity calculations in more detail.⁵¹)

We find that the ν_6 vibrational mode of the linear triplet NC_6N , predicted to be at 1800 cm^{-1} , has the smallest discrepancy from 1848.2 cm^{-1} , which is 48 cm^{-1} . This is a 2.6% difference, which is very close to the observed. In contrast, the other three species have discrepancies of more than 200 cm^{-1} (>11%) and are even larger than the SiC_6Si calculations (Table 5.3). While having a closer value to 1848.2 cm^{-1} is not solid evidence that the observed band is NC_6N , this information could serve as motivation for future work on N-containing

species. Short of performing experiments with nitrogen or oxygen isotopes, there isn't much more analysis that can be done.

In summary, we observed an unidentified absorption at 1848.2 cm^{-1} in the evaporation of 30% Si/ ^{12}C rod. Analysis of ^{13}C isotopic shifts shows that the carrier's structure likely contains a C_6 chain. Because we observed this band in the evaporation of a Si-C rod, there is the possibility that 1848.2 cm^{-1} belongs to a Si-bearing species, making SiC_6Si a reasonable candidate.

Unfortunately, the large discrepancy, between the theoretical prediction for the ν_5 mode of SiC_6Si at 2078 cm^{-1} and the observed value of 1848.2 cm^{-1} , calls this into question. In addition, the presence of a strong C_3O band at 2234 cm^{-1} doesn't allow for a confident Si_nC_m assignment. Four considerations were made in attempting to find an unambiguous identification: (1) repeating experiments to significantly reduce the presence of any contaminants, (2) comparing the DFT predicted isotopic shift patterns of other Si_nC_m species (*e.g.* SiC_7Si , SiC_8Si , etc.) with that of the observed band, (3) examining DFT calculations for SiC_nSi species ($n = 2 - 11$), and finding that the DFT predictions for SiC_6Si doesn't show any unusual behavior, and (4) trying to find a "contaminant-bearing" Si-C species for which DFT calculations predict a vibrational mode close to the observed value of 1848.2 cm^{-1} .

In the end, this project was left with more questions than answers. Despite having repeated experiments to eliminate a contaminant, with a variety of different parameters (*e.g.* laser power, annealing, sintering, etc.), we didn't succeed in eliminating all contaminant species from the sample. DFT calculations were carried out for a variety of Si_nC_m species and contaminant-bearing species to find ones that would produce an isotopic shift pattern similar to that of 1848.2 cm^{-1} . As a result, four contaminant-bearing candidate species were found with a

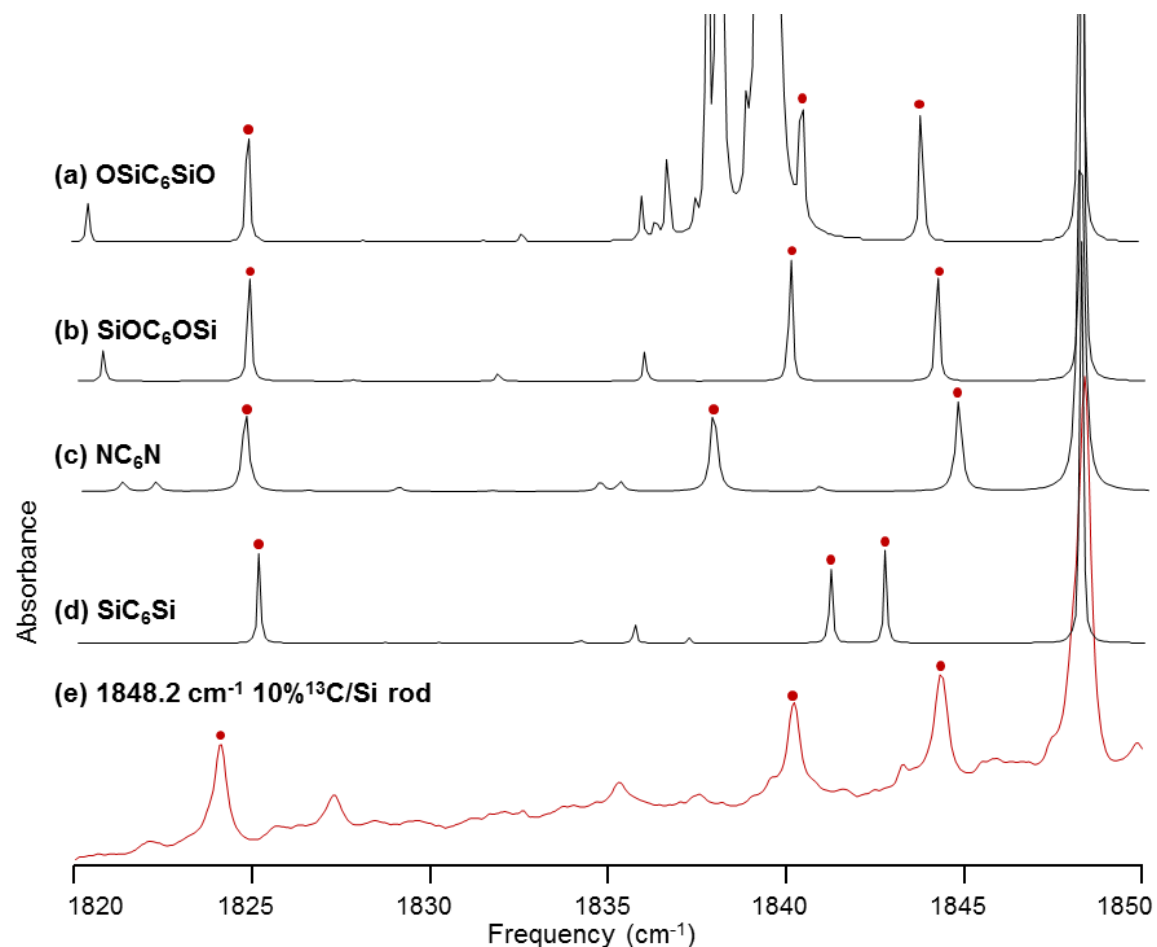


Figure 5.7. A visual comparison of the ^{13}C shift spectra simulated using DFT-B3LYP/cc-pVDZ for (a) OSiC_6SiO , (b) SiOC_6OSi , (c) NC_6N and (d) SiC_6Si with (e) the observed ^{13}C shift spectrum for the 1848.2 cm^{-1} absorption. The singly substituted ^{13}C isotopomer bands are marked by red circles. The simulation in (a) and (d) were calculated using first-order approximation to disable mode-mixing caused by near-lying modes. The discrepancies between simulated and observed shifts are $< 2.3 \text{ cm}^{-1}$. These small discrepancies still leave the question of what carrier is responsible for the 1848.2 cm^{-1} absorption open.

similar pattern, and DFT calculations for the ν_6 mode of NC_6N resulted in a close prediction of 1800 cm^{-1} . In spite of the work done so far, more needs to be done in order to identify the 1848.2 cm^{-1} band.

5.2 THE 1985 - 2065 CM^{-1} REGION

In the experiments that yielded SiC_5 and the unidentified 1848.2 cm^{-1} absorption, other unidentified bands were observed (Figure 5.8) in the region $1985 - 2065\text{ cm}^{-1}$; these are 1992.1 , 1992.9 , 2045.0 and 2060.1 cm^{-1} . This region is very crowded because of near lying bands, as a result, the isotopic shift patterns of these unidentified bands overlap with each other and with that of C_3 and C_9 fundamentals. Experiments were repeated and factors such as laser power, laser focus, rod composition, and sintering were varied with the goal of producing spectra that would allow the unambiguous identification of these isotopomers bands. For example, with the intent of minimizing the production of C_n only molecules, and maximizing that of Si_nC_m molecules, rods were made with a moderately high concentration of silicon, $\sim 30\%$ by mol. 30% by mol was the highest enrichment we could use, because, given the strength of the press and die used to make these rods, higher percentages resulted in rods too fragile to withstand laser ablation. A potential project would be to build some equipment that would allow for the production of high Si enriched rods. Experiments with a high Si:C ratio would minimize the yield of C_n absorptions and optimize the yield of Si_nC_m absorptions in this popular C-C stretching region. Another attempt to minimize the production of long-chain, carbon molecules, involved using a low laser power and tight laser focus with single and double rod ablations. Unfortunately, these experiments did not yield any new information on these unidentified absorptions, except for the 1991.2 cm^{-1} absorption.

Figure 5.9(c) shows a spectrum where the intensity of the 1991.2 cm^{-1} band was optimized, and the intensity of near-lying bands was reduced, allowing for identification of some candidate isotopomer bands. These candidate isotopomer bands are 1987.9 , 1982.3 , 1977.5 , 1967.3 , and probably (because it coincides with a C_3 shift), 1959.9 cm^{-1} . However, this isotopic shift pattern did not match the DFT simulated isotopic shift patterns of a variety of SiC_n ($n = 3-9$). Thus the carrier of 1991.2 cm^{-1} remains unknown.

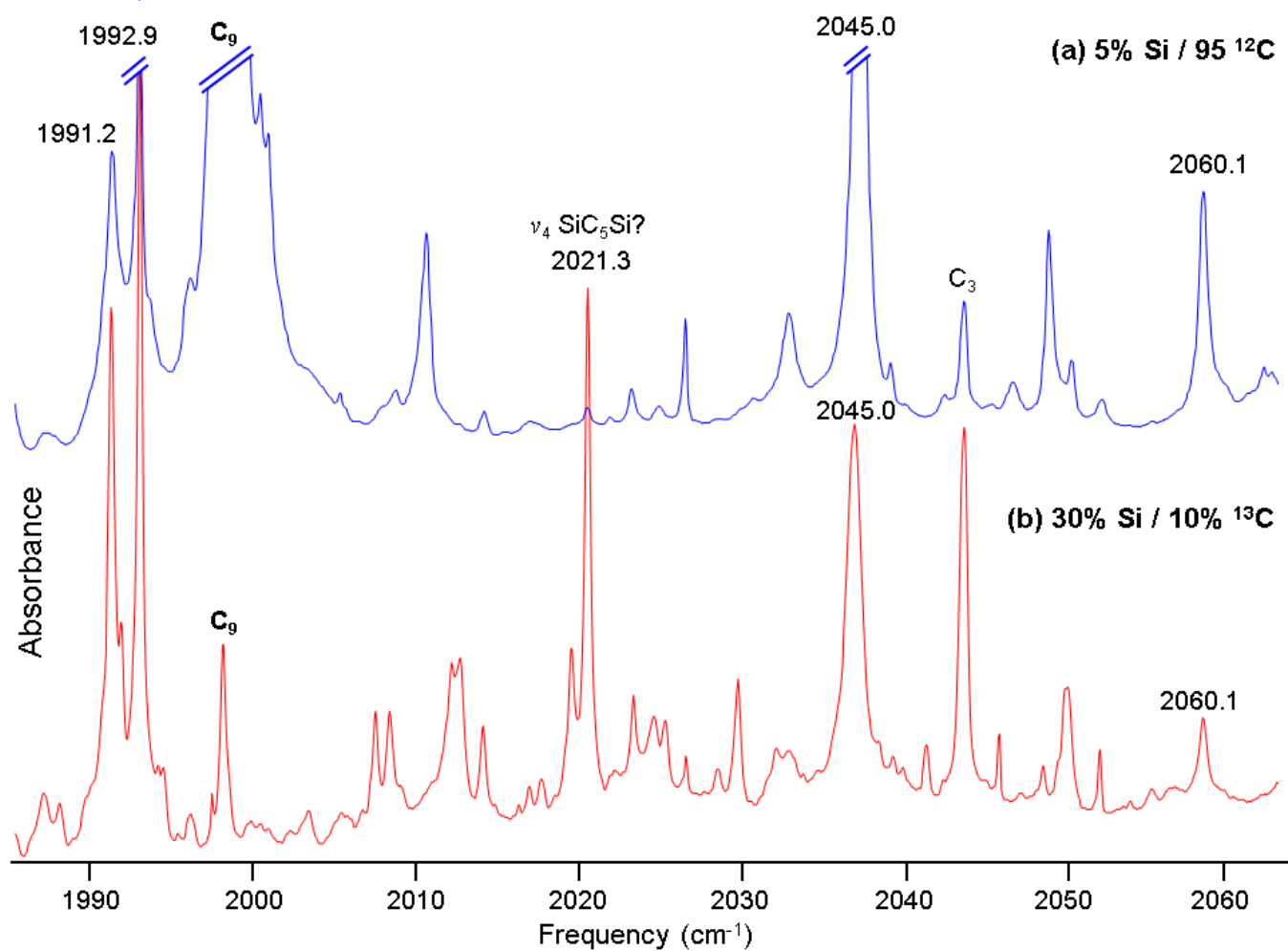


Figure 5.8 Comparison of spectra in the region 1885-2065 cm^{-1} produced from the laser ablation of (a) 5% Si / 95% ^{12}C rod and (b) a 30% Si/ 10% ^{13}C rod. There are four potential Si_nC_m bands at 1992.1, 1992.9, 2045.0 and 2060.1 cm^{-1} , and the spectrum in (b) shows how challenging it is to disentangle and correctly assign the ^{13}C shifts to a specific species.

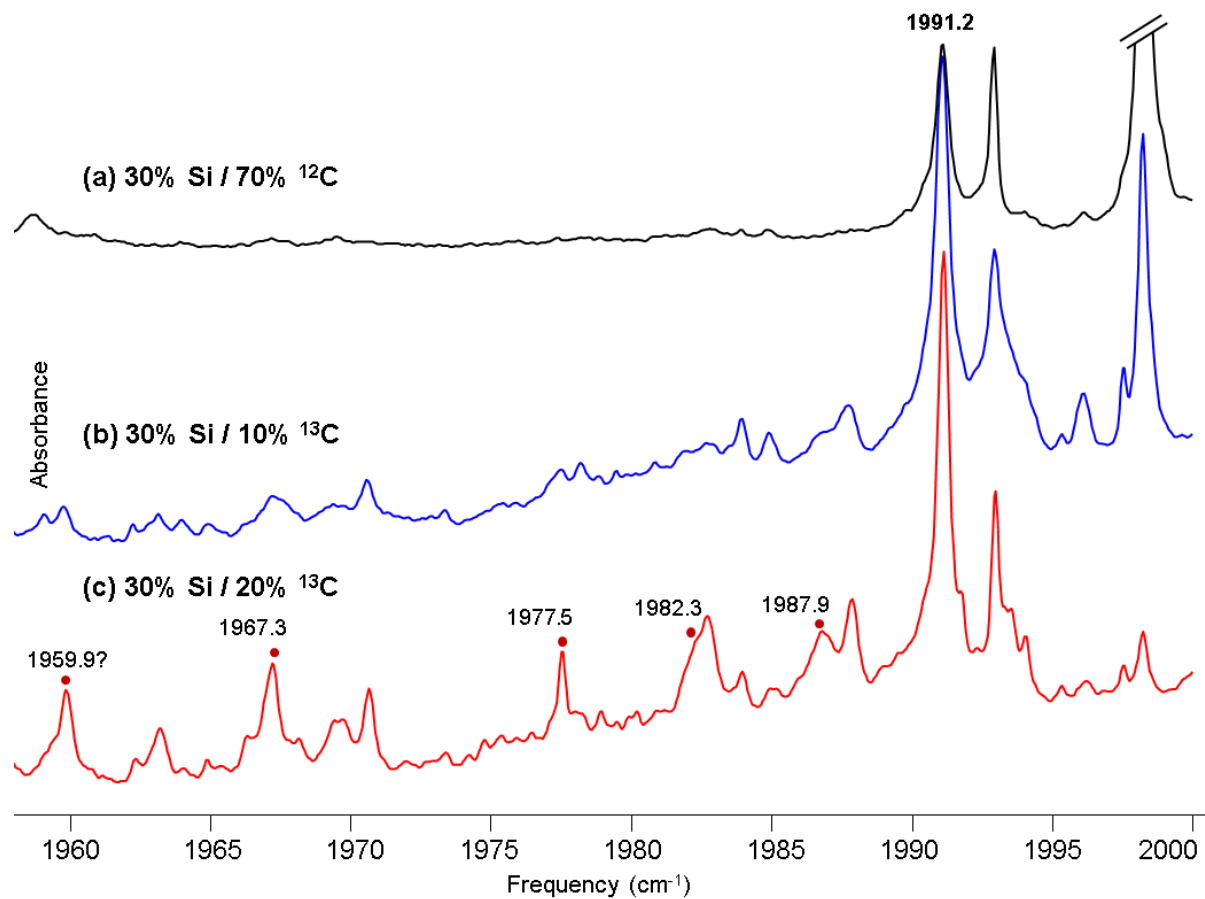


Figure 5.9. Comparison of spectra in the region $1558\text{-}2000\text{ cm}^{-1}$ produced from the laser ablation of (a) 30% Si / 70% ^{12}C rod, (b) a 30% Si/ 10% ^{13}C rod and (c) a 30% Si/ 20% ^{13}C rod. The candidate isotopomer bands for the 1991.2 cm^{-1} fundamental are marked by red circles. There is a “?” for the 1959.9 cm^{-1} because it coincides with the ^{13}C , triply-substituted C_3 isotopomer band.

CHAPTER VI

CONCLUSIONS AND FUTURE WORK

6.1 INTRODUCTION

Linear SiC_n molecules have been detected in interstellar space^{3-12,14} and Si_2C_n molecules are thought to have a role in the formation of silicon carbide grains in meteorite samples, and probably produced in the dust driven wind from pulsating carbon-rich asymptotic giant branch stars.⁸⁶ New spectroscopic information on these species will likely aid future astronomical observations and high resolution gas phase laboratory measurements. This dissertation presents new infrared spectroscopic information that will likely aid future astronomical observations and high resolution gas phase laboratory measurements. In chapters III and IV, we reported on the FTIR measurements and DFT calculations on two novel silicon-carbon species. These molecules have been made by depositing the products of laser evaporation of mixed Si-C rods in solid Ar onto a cold, gold plated mirror, kept at $\sim 20\text{K}$. By finding good agreement between FTIR⁸⁶ measurements and DFT B3LYP/cc-pVDZ calculations of vibrational fundamentals and ^{29,30}Si and ¹³C isotopic shifts, we ascertained the composition and molecular structures. This chapter summarizes the results and also provides suggestions for potential future work that may aid in furthering investigations of Si_nC_m molecules.

6.2 LINEAR SiC_5

The molecule SiC_5 has only been previously detected using FTMW spectroscopy by McCarthy *et al.* in the products formed by reacting silane and acetylene. In this dissertation, we reported on the first identification of a vibrational fundamental of linear triplet SiC_5 , the $\nu_4(\sigma) = 936.9\text{ cm}^{-1}$. This was made possible by the excellent agreement between the observed ^{29,30}Si and

^{13}C -isotopic shifts and DFT predictions. These results were presented at the 66th International Symposium on Molecular Spectroscopy, Ohio State University, Columbus, Ohio, June 2011. They were published in the Journal of Chemical Physics: T.H.Le, C.M.L Rittby, W.R.M Graham, *Fourier transform infrared isotopic study of SiC₅: Identification of the ν_4 mode*. J. Chem. Phys. **140**, 6 (2014).

6.3 LINEAR SiC₅Si

The first FTIR identification of the ν_5 fundamental of linear singlet SiC₅Si has been reported here, along with the tentative assignment for the ν_4 fundamental. The only previous report of Si₂C₅ has been mass spectrometric evidence that was observed by Kaiser *et al.* after reacting the vapor from the ablation of a Si rod with acetylene carrier gas. The unambiguous ν_5 assignment was made by the strong agreement between observed and DFT calculations of $^{29,30}\text{Si}$ and ^{13}C isotopic shifts. In addition, DFT predicts the ν_4 mode to have stronger intensity than ν_5 , and to lie in the crowded C-C stretching region, $\sim 2000\text{ cm}^{-1}$. A tentative identification was made at 2021.3 cm^{-1} , based upon finding potential candidates for ^{13}C isotopomer bands. The near-lying, unidentified bands at 1991.2 , 1992.9 and 2045.0 cm^{-1} cause overlying, isotopic shift patterns, and prevent the unambiguous identification of the isotopomer bands that belong to the carrier of 2021.3 cm^{-1} .

This work has been submitted for publication to the Journal of Chemical Physics.

6.4 FUTURE WORK

The main goal of future work is the identification of new vibrational fundamentals and the production of novel Si_{*n*}C_{*m*} molecules. There are several research leads towards this experimental goal: ascertaining tentative identifications or previously observe unidentified bands, and fabricating rods with high Si enrichment.

6.4.1. *Identification of the Carriers for Unidentified Bands*

In chapter V, the carrier of the 1848.2 cm^{-1} absorption remains unknown. Work that was carried out to try to identify this molecule was discussed in detail and may provide motivation for a project on N-containing species. Moreover, Chapter V discusses a set of unidentified potentially Si-bearing molecules in the region $1975 - 2065\text{ cm}^{-1}$, which is a crowded C-C stretching region. These bands are 1992.1 , 1992.9 , 2045.0 and 2060.0 cm^{-1} and were observed in the condensed products from the laser evaporation of a mixed 30% Si/ 70% ^{12}C rod. These bands do not appear to be correlated with the observed frequencies of identified Si_nC_m molecules and thus will not belong to those molecules.

6.4.2. *Producing Rods with Higher Si Enrichment*

One of the strategies in Si-C molecule production is the optimization of Si-bearing molecules and minimization of C_n -only molecules. This would be very helpful for analysis of observed, unidentified vibrational modes in the crowded C-C stretching region (~ 1900 - 2000 cm^{-1}), where, the isotopomer bands and fundamentals of C_n molecules often overlap that of Si_nC_m molecules. Previous laser ablation experiments done in this lab have used Si enriched rods of no higher than 30% by mol, because higher concentrations result in very fragile rods. This is a potential project that can help spectra with a less crowded C-C stretching region and possibly enable identification of more vibrational fundamentals Si_nC_m .

REFERENCES

- ¹ L. Ziurys and A. Apponi, AIP Conf. Proc. **636**, 154 (2002).
- ² *Molecules in Space*. Retrieved December 2013 from the Cologne Database for Molecular Spectroscopy (CDMS) at http://www.ph1.uni-koeln.de/vorhersagen/molecules/main_molecules.html. The main page is at <http://www.ph1.uni-koeln.de/vorhersagen/>.
- ³ P.W. Merrill, Publ. Astron. Soc. Pac. **38**, 175 (1926).
- ⁴ R. F. Sanford, Publ. Astron. Soc. Pac. **38**, 177 (1926).
- ⁵ R. Klemm, Astrophys. J. **123**, 162 (1956).
- ⁶ R. A. Shepherd and W. R. M. Graham, J. Chem. Phys. **82**, 11 (1985).
- ⁷ V.E. Bondybey, J. Phys. Chem. **86**, 3396 (1982).
- ⁸ J.D. Presilla-Márquez, W.R.M. Graham, R.A. Shepherd, J. Chem. Phys. **93**, 5424 (1990).
- ⁹ T.J. Butenhoff and E.A. Rohlfing, J. Chem. Phys. **95**, 1 (1991).
- ¹⁰ M. Ohishi, N. Kaifu, K. Kawaguchi, A. Murakami, S. Saito, S. Yamamoto, S. Ishikawa, Y. Fujita, Y. Shiratori, and W. M. Irvine, Astrophys. J. **345**, L83 (1989).
- ¹¹ P. F. Bernath, S. A. Rogers, L. C. O'Brien, C. R. Brazier, and A. D. McLean, Phys. Rev. Lett. **60**, 197 (1988).
- ¹² J. Cernicharo, C. A. Gottlieb, M. Guélin, P. Thaddeus, and J. M. Vrtilek, Astrophys. J. **341**, L25 (1989).
- ¹³ M. E. Jacox, NIST Vibrational and Electronic Energy Level Database (<http://webbook.nist.gov/chemistry/>).

- ¹⁴ M. C. McCarthy, A.J. Apponi, C.A. Gottlieb, and P. Thaddeus, *Astrophys. J.* **538**, 766 (2000).
- ¹⁵ A. Nakajima, T. Taguwa, K. Nakao, M. Gomei, R.Kishi, S. Iwata and K. Kaya, *J. Chem. Phys.* **103**, 2500 (1995).
- ¹⁶ J.D. Presilla-Màrquez and W.R.M. Graham, *J. Chem. Phys.* **95**, 5612 (1991).
- ¹⁷ J.D. Presilla-Màrquez, S.C. Gay, C.M.L. Rittby, and W.R.M. Graham, *J. Chem. Phys.* **102**, 6354 (1995).
- ¹⁸ J.D. Presilla-Màrquez and W.R.M. Graham, *J. Chem. Phys.* **96**, 6509 (1992).
- ¹⁹ J.D. Presilla-Màrquez and W.R.M. Graham, *J. Chem. Phys.* **100**, 181 (1994).
- ²⁰ J.D. Presilla-Màrquez, C.M.L. Rittby, and W.R.M. Graham, *J. Chem. Phys.* **104**, 2818 (1996).
- ²¹ J.D. Presilla-Màrquez, C.M.L. Rittby, and W.R.M. Graham, *J. Chem. Phys.* **106**, 8367 (1997).
- ²² X. D. Ding, S. L. Wang, C. M. L. Rittby, and W. R. M. Graham, *J. Chem. Phys.* **110**, 11214 (1999).
- ²³ X. D. Ding, C. M. L. Rittby, and W. R. M. Graham, *J. Phys. Chem. A* **104**, 3712 (2000).
- ²⁴ M. E. Jacox, *Chem. Soc. Rev.* **31**, 108 (2002).
- ²⁵ A. Van Orden, R. A. Provencal, T. F. Giesen, and R. J. Saykally, *Chem. Phys. Lett.* **237**, 77 (1995).
- ²⁶ A. Van Orden, T. F. Giesen, R. A. Provencal, H. J. Hwang, and R. J. Saykally, *J. Chem. Phys.* **101**, 10237 (1994).
- ²⁷ M. C. McCarthy, C.A. Gottlieb, and P. Thaddeus, *Mol. Phys.* **101**, 797 (2003).

- ²⁸ M. Pellarin, C. Ray, P. Mélinon, J. Lermé, J. L. Vialle, P. Kéghélian, A. Perez, and M. Broyer, *Chem. Phys. Lett.* **277**, 96 (1997).
- ²⁹ S. Hunsicker and R. O. Jones, *J. Chem. Phys.* **105**, 12 (1996).
- ³⁰ M. Bertolus, V. Brenner, and P. Millié, *Eur. Phys. J. D* **1**, 197 (1998).
- ³¹ P. Botschwina and R. Oswald, *Zeitschrift für Physikalische Chemie*, **215**, 3, 393 (2001).
- ³² Z. Jiang, X. Xu, H. Wu, F. Zhang, Z. Jin, *Theochem-J. Mol. Struct.* **103**, 589 (2002).
- ³³ J.L. Deng, K.H. Su, X. Wang, Q.F. Zeng, L.F. Cheng, Y.D. Xu, and L.T. Zhang. *Eur. Phys. J. D* **49**, 21 (2008).
- ³⁴ R.I. Kaiser, P. Maksyutenko, C. Ennis, F. Zhang, X. Gu, S.P. Krishtal, A.M. Mebel, O. Kostkoc and Musahid Ahmed, *Faraday Discuss*, **147**, 429 (2010).
- ³⁵ Z. Jiang, X. Xu, H. Wu, F. Zhang, Z. Jin, *Theochem-J. Mol. Struct.* **103**, 589 (2002).
- ³⁶ M. Gomei, R. Kishi, and A. Nakajima, S. Iwata, and K. Kaya, *J. Chem. Phys.* **107**, 23 (1997).
- ³⁷ M. C. McCarthy, A. J. Apponi, C. A. Gottlieb, and P. Thaddeus, *Astrophys. J.* **538**, 766 (2000).
- ³⁸ A. J. Apponi, M. C. McCarthy, C. A. Gottlieb, and P. Thaddeus, *Astrophys. J. Lett.* **516**, L103 (1999).
- ³⁹ M. Ohishi, N. Kaifu, K. Kawaguchi, A. Murakami, S. Saito, S. Yamamoto, S. Ishikawa, Y. Fujita, Y. Shiratori, and W. M. Irvine, *Astrophys. J.* **345**, L83 (1989).
- ⁴⁰ G. E. Davico, R. L. Schwartz and W. C. Lineberger, *J. Chem. Phys.* **115**, 1789 (2001).

- ⁴¹ J. M. Rintelman, M. S. Gordon, G. D. Fletcher, and J. Ivanić, *J. Chem. Phys.* **124**, 034303 (2006).
- ⁴² A. J. Apponi, M. C. McCarthy, C. A. Gottlieb, and P. Thaddeus, *J. Chem. Phys.* **111**, 3911 (1999).
- ⁴³ M. C. McCarthy, A. J. Apponi, and P. Thaddeus, *J. Chem. Phys.* **111**, 7175 (1999).
- ⁴⁴ P. A. Withey and W. R. M. Graham, *J. Chem. Phys.* **96**, 4068 (1992).
- ⁴⁵ N. Moazzen-Ahmadi and F. Zerbetto, *Chem. Phys. Lett.* **164**, 517 (1989).
- ⁴⁶ A. Van Orden, R. G. Provençal, T. F. Giesen, and R. J. Saykally, *Chem. Phys. Lett.* **237**, 77 (1995).
- ⁴⁷ V. D. Gordon, E. S. Nathan, A. J. Apponi, M. C. McCarthy, P. Thaddeus and P. Botschwina, *J. Chem. Phys.* **113**, 5311 (2000).
- ⁴⁸ H. Sun, H. Gong, H. Liu, F. Wang, X. Pan, Z. Su, C. Sun, R. Wang, X. Huang, *Theor. Chem. Acc.* **126**, 15 (2010).
- ⁴⁹ M. L. Senent, R. Domínguez-Gómez, *Chem. Phys. Lett.* **501**, 25 (2010).
- ⁵⁰ X. D. Ding, C. M. L. Rittby, and W. R. M. Graham, *J. Phys. Chem. A* **104**, 3712 (2000).
- ⁵¹ X. D. Ding, S. L. Wang, C. M. L. Rittby, and W. R. M. Graham, *J. Chem. Phys.* **110**, 11214 (1999).
- ⁵² Z. Jiang, X. Xu, H. Wu, F. Zhang, Z. Jin, *Theochem-J. Mol. Struct.* **589**, 103 (2002).
- ⁵³ H. Zhan, W. Cai, Q. Guo, X. Shao, *Chem. Phys. Lett.* **405**, 97 (2005).
- ⁵⁴ C. M. L. Rittby (private communication on unpublished calculations).

- ⁵⁵ M. Bertolus, V. Brenner, and P. Millié, *Eur. Phys. J. D* **1**, 197 (1998).
- ⁵⁶ P. Botschwina and R. Oswald, *Zeitschrift für Physikalische Chemie*, **215**, 3, 393 (2001).
- ⁵⁷ J.L. Deng, K.H. Su, X. Wang, Q.F. Zeng, L.F. Cheng, Y.D. Xu, and L.T. Zhang. *Eur. Phys. J. D* **49**, 21 (2008).
- ⁵⁸ L.N. Shen, T.J. Doyle and W.R.M Graham, *J. Chem. Phys.* **93**, 1597 (1990).
- ⁵⁹ A. D. Becke, *Phys. Rev. A* **38**, 3098 (1988).
- ⁶⁰ J.P. Perdew, *Phys. Rev. B* **33**, 8822 (1986).
- ⁶¹ C. Lee, W. Yang, and R. G. Parr, *Phys. Rev. B* **37**, 785 (1988).
- ⁶² R. I. Kaiser, P. Maksyutenko, C. Ennis, F. Zhang, X. Gu, S. P. Krishtal, A. M. Mebel, O. Kostkoc, and M. Ahmed, *Faraday Discuss.* **147**, 429 (2010).
- ⁶³ Y. Yasuda and T. Kozasa, *Astrophys. J.* **745**, 159 (2012).
- ⁶⁴ W. Weltner, Jr. and D. Mcleod, Jr., *J. Chem. Phys.* **41**, 235 (1964).
- ⁶⁵ J. D. Presilla-Márquez and W. R. M. Graham, *J. Chem. Phys.* **95**, 5612 (1991).
- ⁶⁶ Z. H. Kafafi, R. H. Hauge, L. Fredin, and J. Margrave, *J. Phys. Chem.* **87**, 797 (1983).
- ⁶⁷ C. M. L. Rittby, *J. Chem. Phys.* **95**, 5609 (1991).
- ⁶⁸ J. D. Presilla-Márquez, S. C. Gay, C. M. L. Rittby, and W. R. M. Graham *J. Phys. Chem.* **102**, 6354 (1995).
- ⁶⁹ J. D. Presilla-Márquez, and W. R. M. Graham, *J. Chem. Phys.* **100**, 181 (1994).
- ⁷⁰ J. D. Presilla-Márquez, and W. R. M. Graham, *J. Chem. Phys.* **100**, 181 (1994).
- ⁷¹ C. M. L. Rittby, *J. Chem. Phys.* **100**, 175 (1994).

- ⁷² A. Van Orden, T. F. Giesen, R. A. Provençal, H. J. Hwang, and R. J. Saykally, *J. Chem. Phys.* **101**, 10237 (1994).
- ⁷³ X. Duan, L.W. Burggraf, D. E. Weeks, G. E. Davico, R.L. Schwartz, and W. C. Linberger, *J. Chem. Phys.* **116**, 3601 (2002).
- ⁷⁴ S. Thorwirth, J. Krieg, V. Lutter, I. Keppeler, S. Schlemmer, M. E. Harding, J. Vázquez, and T. F. Giesen, *J. Mol. Spec.* **270**, 75 (2011).
- ⁷⁵ G. Froudakis, A. Zdetsis, M. Mühlhäuser, B. Engels, and S. D. Peyerimhoff, *J. Chem. Phys.* **101**, 6790 (1994).
- ⁷⁶ C. Lee, W. Yang, and R. G. Parr, *Phys. Rev. B* **37**, 785 (1988).
- ⁷⁷ B. Miehlich, A. Savin, H. Stoll, and H. Preuss, *Chem. Phys. Lett.* **157**, 200 (1989).
- ⁷⁸ A. D. Becke, *J. Chem. Phys.* **98**, 5648 (1993).
- ⁷⁹ Z. Jiang, X. Xu, H. Wu, F. Zhang, and Z. Jin, *Theochem-J. Mol. Struct.* **589**, 103 (2002).
(There is a misprint in Table 4 where the molecules are listed as Si_2C_m but are actually $\text{Si}_2\text{C}_{m-2}$.)
- ⁸⁰ L. N. Shen, T. J. Doyle, and W. R. M. Graham, *J. Chem. Phys.* **93**, 1597 (1990).
- ⁸¹ A. D. Becke, *Phys. Rev. A* **38**, 3098 (1988).
- ⁸² J.P. Perdew, *Phys. Rev. B* **33**, 8822 (1986).
- ⁸³ T. H. Dunning, Jr., *J. Chem. Phys.* **90**, 1007 (1989).
- ⁸⁴ R.H. Kranze, W.R.M. Graham, *J. Chem. Phys.* **98**, 1, 71 (1993)
- ⁸⁵ M. Vala, T.M. Chandrasekhar, J. Szczepanski, R. Pellow, *High Temp. Sci.*, **27**, 19 (1988)
- ⁸⁵ Y. Yasuda and T. Kozasa, *Astrophys. J.* **745**, 159 (2012).

VITA

Personal	Christina “Tina” Huong Lê
Background	Born on 15 November 1986, San Jose, CA Eldest daughter of Rohvenson Le and Que Ninh
Education	Diploma, Adrian Wilcox High School, Santa Clara, CA, 2004. B.A., Physics, Reed College, Portland, OR, 2008. Ph.D., Physics, Texas Christian University, Ft. Worth, TX, 2014.
Experience	Research Assistant, San Jose State University, Research Experience for Undergraduates (REU), Summer 2006 Research Thesis Senior, Reed College, August 2007 – May 2008 Teaching Assistant, Texas Christian University, August 2008 - 2013 Research Assistant, TCU Molecular Physics Laboratory, Texas Christian University, August 2008 - present
Memberships	American Physical Society and Toastmasters International
Awards	Student Research Symposium Graduate Presentation Award (2011) Student Research Symposium Teaching Assistant Award (2010)
Publications	T.H. Lê, C. M. L. Rittby, and W. R. M. Graham, <i>Fourier transform infrared isotopic study of SiC₅: Identification of the ν_4 mode</i> . J. Chem. Phys. 140 , 6 (2014). T. H. Lê, C. M. L. Rittby, and W. R. M. Graham, <i>Fourier transform infrared identification of the ν_5 fundamental of SiC₅Si</i> . J. Chem. Phys., <i>in preparation</i> (2014).

ABSTRACT

FOURIER TRANSFORM INFRARED SPECTROSCOPIC AND DENSITY FUNCTIONAL THEORETICAL STUDIES OF SILICON-CARBON MOLECULES

by Tina Huong Lê, Ph.D. 2014
Department of Physics and Astronomy
Texas Christian University

Dissertation Co-Advisors:

Dr. W. R. M. Graham, Professor of Physics and Astronomy, Chair of the Department
Dr. C. M. L. Rittby, Professor of Physics and Astronomy, Associate Dean of CSE

Astronomers, experimentalists and theorists have produced a great deal of research on Si_nC_m species, because of their potential applications to astrophysics and the study of Group IV molecules. The present work is part of this on-going research and we report here, the synthesis and observation of vibrational fundamentals of silicon-carbon species, SiC_5 and SiC_5Si .

The infrared spectrum of SiC_5 was observed by trapping the vapor from the Nd:YAG laser ablation of sintered Si/C rods in solid Ar at ~ 20 K. Measurements of ^{13}C and $^{29,30}\text{Si}$ isotopic shifts have enabled the identification of the $\nu_4(\sigma)$ vibrational fundamental of the linear isomer of SiC_5Si at $936.9 \pm 0.2 \text{ cm}^{-1}$. The observed isotopic shifts are in excellent agreement with the predictions of DFT (density functional theory) calculations at the B3LYP/cc-pVDZ level.

SiC_5Si was produced using argon matrix trapping and Nd:YAG laser ablation of a sintered 30% Si/ 70% ^{12}C rod in solid Ar at ~ 20 K. The ^{13}C and $^{29,30}\text{Si}$ isotopic shifts were observed, and upon comparison with the calculations of DFT-B3LYP/cc-pVDZ, are in excellent

agreement. This leads to a confident identification of the $\nu_5(\sigma_u)$ fundamental of linear SiC_5Si at $1590.8 \pm 0.2 \text{ cm}^{-1}$. A second fundamental, $\nu_4(\sigma_u)$, can only be tentatively identified at 2021.0 cm^{-1} because near-lying absorptions belonging to other species overlap its isotopic shift pattern.